

Aplastic Anemia Rescued by Exhaustion of Cytokine-secreting CD8⁺ T Cells in Persistent Infection with Lymphocytic Choriomeningitis Virus

By Daniel Binder,^{*‡} Maries F. van den Broek,^{*} David Kägi,^{*} Horst Bluethmann,[§] Jörg Fehr,[‡] Hans Hengartner,^{*} and Rolf M. Zinkernagel^{*}

From the ^{*}Institute of Experimental Immunology, Department of Pathology, University Hospital of Zürich, CH-8091 Zürich, Switzerland; the [‡]Division of Hematology, Department of Internal Medicine, University Hospital of Zürich, CH-8091 Zürich, Switzerland; and the [§]CNS Department, Pharmaceutical Research Gene Technologies, F. Hoffmann–La Roche Ltd., CH-4070 Basel, Switzerland

Summary

Aplastic anemia may be associated with persistent viral infections that result from failure of the immune system to control virus. To evaluate the effects on hematopoiesis exerted by sustained viral replication in the presence of activated T cells, blood values and bone marrow (BM) function were analyzed in chronic infection with lymphocytic choriomeningitis virus (LCMV) in perforin-deficient (P^{0/0}) mice. These mice exhibit a vigorous T cell response, but are unable to eliminate the virus. Within 14 d after infection, a progressive pancytopenia developed that eventually was lethal due to agranulocytosis and thrombocytopenia correlating with an increasing loss of morphologically differentiated, pluripotent, and committed progenitors in the BM. This hematopoietic disease caused by a noncytopathic chronic virus infection was prevented by depletion of CD8⁺, but not of CD4⁺, T cells and accelerated by increasing the frequency of LCMV-specific CD8⁺ T cells in T cell receptor (TCR) transgenic (tg) mice. LCMV and CD8⁺ T cells were found only transiently in the BM of infected wild-type mice. In contrast, increased numbers of CD8⁺ T cells and LCMV persisted at high levels in antigen-presenting cells of infected P^{0/0} and P^{0/0} × TCR tg mice. No cognate interaction between the TCR and hematopoietic progenitors presenting either LCMV-derived or self-antigens on the major histocompatibility complex was found, but damage to hematopoiesis was due to excessive secretion and action of tumor necrosis factor (TNF)/lymphotoxin (LT)-α and interferon (IFN)-γ produced by CD8⁺ T cells. This was studied in double-knockout mice that were genetically deficient in perforin and TNF receptor type 1. Compared with P^{0/0} mice, these mice had identical T cell compartments and T cell responses to LCMV, yet they survived LCMV infection and became life-long virus carriers. The numbers of hematopoietic precursors in the BM were increased compared with P^{0/0} mice after LCMV infection, although transient blood disease was still noticed. This residual disease activity was found to depend on IFN-γ-producing LCMV-specific T cells and the time point of hematopoietic recovery paralleled disappearance of these virus-specific, IFN-γ-producing CD8⁺ T cells. Thus, in the absence of IFN-γ and/or TNF/LT-α, exhaustion of virus-specific T cells was not hampered.

Key words: aplastic anemia • lymphocytic choriomeningitis virus • cytotoxic T lymphocytes • cytokines • immune tolerance

Sustained suppression and/or destruction of pluripotent and committed hematopoietic precursors in the bone marrow (BM)¹ leads to aplastic anemia (AA) (1). Severely

impaired hematopoiesis in the BM and, as a consequence, failure to produce mature blood cells, are usually fatal for the host due to bacterial invasion or bleeding. Apart from

¹Abbreviations used in this paper: aa, amino acids; AA, aplastic anemia; BFU-E, burst-forming unit–erythroid; BM, bone marrow; BSS, balanced salt solution; CBC, cellular blood count; CFU-GM, CFU–granulocyte/macrophage; CFU-Meg, CFU–megakaryocyte; CFU-S, CFU–stem cell; gp,

glycoprotein; LCMV, lymphocytic choriomeningitis virus; LCMV-GP, glycoprotein of LCMV; LT, lymphotoxin; m, murine; NU, neutralizing units; NSS, normal sheep serum; P^{0/0}, perforin-deficient; p.i., post infection; SPF, specific pathogen-free; tg, transgenic; vacc-LCMV-GP, vaccinia virus recombinant expressing LCMV-GP; wild-type, wt.

drugs and chemicals, host genes, autoimmune responses, cytokines, and viruses have been implicated in the initiation and progression of this disorder (for review see reference 2). Most of the known viruses causing human BM failure tend to persistently infect the host and are non- or poorly cytopathic for blood cell progenitors; therefore a major role of destructive immunity in the pathogenesis of the disease has been postulated. Examples of this class of viruses include Epstein-Barr virus (3, 4), cytomegalovirus (5, 6), human immunodeficiency virus (7), and probably the putative viral agent associated with non-A-G posthepatitis AA (8, 9). Furthermore, T cells seem to be important because there is a correlation between susceptibility to AA and certain MHC haplotypes (10, 11) and hematopoietic function improves after immunosuppressive strategies with antilymphocyte sera or syngeneic BM transplantation (12, 13). It is not known, however, whether virus-induced T cell-mediated AA depends on (a) a cognate interaction between T cells and hematopoietic cells presenting a virus-derived T cell epitope on the appropriate MHC, (b) on soluble mediators released from virus-specific T cells, or (c) on loss of tolerance and autoimmune destruction of pluripotent and committed stem cells (14).

We previously investigated innate immune effector mechanisms involved in transient BM aplasia during acute infection with lymphocytic choriomeningitis virus (LCMV) in mice devoid of the IFN- α/β R, IFN- γ R, functional NK cells (perforin-deficient [$P^{0/0}$] mice), Fas (CD95, *lpr*), CD4⁺, or CD8⁺ T cells (15). This study documented that the reversible suppressive effect on hematopoietic precursors in the BM was predominantly mediated by IFN- α/β and that virally induced NK cells either by direct cytolysis and/or secreted factors or LCMV-specific CTLs were not involved at this early stage of infection. Although the non-cytopathic LCMV replicated vigorously in megakaryocytes and myeloid precursors in mice lacking IFN type I R (IFN- α/β R $^{0/0}$), the role of T cells could not be studied in these mice because LCMV-specific CTLs are rapidly exhausted by the overwhelming amounts of viral antigen (16). The murine model infection with LCMV has contributed substantially to the view, however, that T cell-mediated protective immunity is involved in autoimmune and/or immunopathological diseases via a direct cognate cell to cell interaction in tissues that are either infected with LCMV or express the relevant epitopes derived from LCMV (17). Thus, the classical choriomeningitis (18), hepatitis (19), immunosuppression (20) and LCMV-triggered destruction of the islets of Langerhans (21) or oligodendrocytes in the central nervous system expressing the glycoprotein of LCMV (LCMV-GP; reference 22) have been shown to be CD8⁺ T cell mediated and contact dependent. It has been suggested that the permanent release of cytokines secreted by virus-specific T cells during persistent LCMV infection induces cachexia and supports inflammatory processes causing chronic disease, and that both CD4⁺ T helper cells and CD8⁺ CTLs are involved (23–25). The BM may be particularly susceptible to T cell-mediated, cy-

tokine-dependent injury because blood cells, in contrast to solid epithelial organs, must continuously regenerate and their constant levels in the periphery are maintained by asymmetric division from a small number of pluripotent stem cells (26).

We therefore evaluated the respective potential role of CD4⁺ and CD8⁺ T cells and of their released soluble mediators in causing hematopoietic abnormalities during persistent LCMV infection in $P^{0/0}$ mice. These mutant mice were chosen as experimental model because they exhibit a vigorous and continuous LCMV-specific T cell response but are unable to clear the virus (27). Here we report that LCMV-specific CD8⁺ T cells, but not CD4⁺ T cells, caused AA in LCMV-infected $P^{0/0}$ mice. By generating double-knockout mice genetically deficient for perforin and TNFR1 ($P^{0/0}$ /TNFR1 $^{0/0}$) and by using a sheep antiserum neutralizing mouse IFN- γ , LCMV-induced AA was prevented and infected mice became life-long virus carriers through functional exhaustion of virus-specific, IFN- γ -secreting CD8⁺ T cells.

Materials and Methods

Mice. The generation and breeding of $P^{0/0}$, LCMV-GP-specific TCR-transgenic (tg; line 318), $P^{0/0}$ TCR-tg ($P^{0/0}$ \times TCR), and mice expressing the LCMV-GP transgene under the control of the rat insulin promoter have been described previously (21, 27). These mice and C57BL/6 mice as controls were obtained from the breeding colony at the Institut für Versuchstierkunde (University of Zürich, Zürich, Switzerland). Mice lacking TNFR1 (TNFR1 $^{0/0}$ [28]) were bred at the animal facility of F. Hoffmann-La Roche Ltd. (Basel, Switzerland). All mouse strains were kept under specific pathogen-free (SPF) conditions. Sex-matched mice of 8–12 wk of age were used. The animal protection law of the Kanton of Zürich (Zürich, Switzerland) limits the number of mice to be used in experiments, particularly if disease is severe. Therefore, experiments generally were repeated twice with groups of two to four mice.

Breeding of Mice with Double Deficiency for Perforin and TNFR1 ($P^{0/0}$ /TNFR1 $^{0/0}$). TNFR1 $^{0/0}$ mice are homozygous mutant mice that originally were bred by crossing germline transmitters of the mutated TNFR1 allele (129/SvEv, H-2^b) with C57BL/6 (H-2^b) mice. These single-knockout mice were crossed with $P^{0/0}$ mice (pure C57BL/6 background) and the resulting F1 generation with heterozygosity for both alleles (TNFR1 and perforin) was interbred to yield homozygous double-knockout F2 offsprings ($P^{0/0}$ /TNFR1 $^{0/0}$). The F2 generation displayed the expected mendelian 1:16 frequency of homozygous $P^{0/0}$ /TNFR1 $^{0/0}$ mice, indicating that these mice are fertile and breed normally; in addition, they have no apparent phenotypic abnormalities and have a normal life span. Homozygous $P^{0/0}$ /TNFR1 $^{0/0}$ mice were identified by the presence of both mutated alleles, determined with PCR using two different primer pairs for each, perforin and TNFR1, respectively, on DNA prepared from tail biopsies. The first pair (5'-TTT TTG AGA CCC TGT AGA CCC A-3', 5'-GCA TCG CCT TCT ATC GCC TTC T-3') detecting the perforin genotype yields a band of 665 bp for the mutated and is negative for the wild-type (wt) allele, the second pair (5'-CCG GTC CTG AAC TCC TGG CCA A-3', 5'-CCC CTG CAC ACA TTA CTG GAA G-3') yields a 300-bp fragment for the wt and a

1,300-bp fragment for the mutated allele. The TNFR1 genotype was determined with a first pair detecting the neo cassette (5'-GTT AGG TCT CTC CTG AAT GTG ATC-3', 5'-TCC CGC TTC AGT GAC AAC GTC-3'), which results in a 2,000-bp fragment for the mutated and is negative for the wt allele; the second pair (5'-CTC TCT TGT GAT CAG CAC TG-3', 5'-CTG GAA GTG TGT CTC AC-3') yields a 1,400-bp fragment for the wt and a 2,000-bp fragment for the mutated allele.

Virus. LCMV-WE, originally obtained from Dr. F. Lehmann-Grube (Pette Institut, Hamburg, Germany; reference 29), was used in all experiments and mice were always infected with 200 PFU intravenously. Second passage virus derived from plaque-purified isolates was propagated on L929-fibroblast cells. The virus was titrated using an immunological focus assay that is two- to threefold less sensitive than virus titers detected by *in vivo* infection (30). LCMV titers are expressed as \log_{10} of PFU/ml (blood), \log_{10} of PFU/ 10^7 nucleated cells (BM), or as \log_{10} of PFU/g of tissue (solid organs). Recombinant vaccinia virus expressing LCMV-GP (vacc-LCMV-GP) was a gift from Dr. D.H.L. Bishop (Institute of Virology, Oxford University, Oxford, UK). Recombinant vaccinia virus stocks were grown on BSC 40 cells. The cells and culture supernatants were collected 2 d after infection, subjected to three cycles of freezing and thawing, sonicated on ice for 30 s, and centrifuged.

Peripheral Blood Values and BM Cytology. Blood samples (40 μ l diluted 1:5) were obtained from the retrobulbar plexus of ether-anesthetized mice and cellular blood counts (CBCs) were determined in a hemocytometer (TECHNICON H2[®]; Technicon Instruments Corp., Tarrytown, NY). Differential white blood cell counts were defined microscopically by scoring blood smears stained with May-Grünwald/Giemsa. Reticulocyte counts were quantitated by flow cytometry (SYSMEX R-3000[®]; Toa Medical Electronics, Kobe, Japan). Differential counts of BM cells were determined on May-Grünwald/Giemsa, Sudan black B, myeloperoxidase, chloracetate esterase, or α -naphthyl butyrate esterase stained smears. For immunocytochemical detection of LCMV, BM smears on slides were fixed in acetone and stained with the rat anti-LCMV mAb VL-4 as described (15). CD11c on dendritic cells was stained with the hamster mAb N418 (HB-224; American Type Culture Collection, Rockville, MD). Primary hamster Igs were detected by alkaline-phosphatase-labeled rabbit anti-hamster Ig followed by alkaline-phosphatase-labeled goat anti-rabbit Ig.

Pluripotent and Committed Progenitor Assays. Pluripotent and committed hematopoietic progenitors were determined as described before (15). In brief, recipient mice were immunized with 10^2 PFU of LCMV. 2 wk later they were lethally irradiated (900 cGy) and reconstituted intravenously with 10^4 – 10^5 syngeneic BM cells from infected or uninfected control mice. 12 d after irradiation, the spleens of the recipient mice were fixed in Tellesnick's fixative and individual colonies on the spleen surface (colony-forming unit-stem cells [CFU-S]) were counted under a dissecting microscope. Cell suspensions from BM in isotonic balanced salt solution (BSS) were counted and assessed for viability by trypan blue exclusion before testing *in vitro* for colony formation. The culture mixture was prepared in IMDM supplemented with 5×10^{-5} mol/liter 2-mercaptoethanol, penicillin-streptomycin, 0.9% methylcellulose, 30% FCS, and 1% BSA in the presence of optimized concentrations of growth factors (murine [m]IL-3 [30 U/ml] and mGM-CSF [30 U/ml] for CFU-granulocyte/macrophage [CFU-GM]; mIL-3 [30 U/ml] and human erythropoietin [5 U/ml] for burst-forming unit-erythroid [BFU-E]; and mIL-3 [30 U/ml] and murine thrombopoietin [mTPO; 500 ng/ml] for

CFU-megakaryocyte [CFU-Meg]). Recombinant murine IL-3 and GM-CSF were obtained from PharMingen Inc. (San Diego, CA), recombinant human erythropoietin was purchased from Cilag AG (Schaffhausen, Switzerland), and recombinant mTPO was a gift from Genentech Inc. (South San Francisco, CA). Individual colonies were scored by morphology after 5–7 d (CFU-Meg), 7 d (CFU-GM), or 8 d (BFU-E). The total number of colonies per femur was calculated using the cellularity obtained for the individual BM.

Antiserum Treatment of Mice. Monoclonal rat anti-mouse CD4 (YTS 191.1) and monoclonal rat anti-mouse CD8 (YTS 169.4) were originally obtained from Dr. H. Waldmann (Dunn School of Pathology, Oxford, UK; reference 31). Thymectomized mice were injected intravenously with 2 mg of the appropriate mAb 3 and 1 d before LCMV infection. Efficacy of treatment was checked by FACS[®] (Becton Dickinson, Mountain View, CA) analysis. The production of sheep anti-mouse IFN- γ antiserum has been described (32). After partial purification of pooled sera by $(\text{NH}_4)_2\text{SO}_4$ precipitation, neutralizing titers of 5×10^4 neutralizing units (NU)/ml were obtained. Mice were treated daily from day 5 to day 15 after LCMV infection with 2×10^4 NU anti-IFN- γ in 0.2 ml of BSS intraperitoneally. Control mice were injected with normal sheep serum.

Cytotoxicity Assay. CTL activity of spleen cells was determined by a ^{51}Cr -release assay as described (33). In brief, mice were infected intravenously 8 d before with 200 PFU of LCMV. Single spleen cell suspensions were prepared at 7×10^6 /ml in MEM + 2% FCS. Fibroblast target cells MC57G (H-2^b) or T cell lymphoma target cells RMA (H-2^b) were coated with LCMV-GP-derived immunodominant peptide amino acids (aa)33-41 (glycoprotein [gp]33) at a concentration of 10^{-6} M, and were labeled with 1 μCi of $\text{Na}^{51}\text{CrO}_4$ for 2 h at 37°C, washed three times, and resuspended at 10^5 /ml. Threefold dilutions of spleen cells were incubated with 100 μ l of target cells in 96-well microtiter round-bottomed plates for 5 h. A total of 70 μ l of the supernatant was assayed for released ^{51}Cr . The percent specific release of ^{51}Cr was calculated as [(experimental release – spontaneous release) \times 100/(total release – spontaneous release)]. Spontaneous release was always <20%.

Analysis of Secreted Cytokines by LCMV-specific T Cells. Mice were immunized intravenously with 200 PFU LCMV-WE. 8 or 14 d later, CD8⁺ T cells were purified from spleen cell suspensions by MACS[®] sorting according to the protocol of the supplier (Miltenyi Biotec, Bergisch Gladbach, Germany); the proportion of pure CD8⁺ T cells obtained was in the range of 70–85%. 10^5 CD8⁺ T cells were incubated in 96 wells with threefold serial dilutions of gp33 in concentrations ranging from 10^{-6} to 10^{-8} M or medium only (RPMI, FCS 5%, with Con A supernatant 2%) in the presence of 6×10^5 irradiated (2,000 cGy) C57BL/6 spleen cells. 48 h later supernatants were analyzed for IFN- γ and TNF/lymphotoxin (LT)- α by ELISA as described (34).

Flow Cytometry. Single-cell suspensions of BM, thymus, or spleen were prepared at 4°C in buffer solution (BSS containing 2% FCS and 0.2% NaN_3) for staining with mAbs conjugated with fluorochromes. The following antibodies were used: anti-CD4 and anti-CD8 (Becton Dickinson), anti-TCR V α 2, anti-IFN- γ , and anti-TNF/LT- α (PharMingen). To detect expansion of gp33-specific TCR-tg T cells in the BM, cell suspensions were doubly stained with a PE-conjugated V α 2-specific mAb and FITC-conjugated anti-CD8-specific mAb. After lysis of erythrocytes with FACS[®] lysis solution and washing, cell suspensions were analyzed on a FACScan[®] using logarithmic scales. To detect intracellular cytokines, MACS[®]-enriched CD8⁺ T cells were

stimulated with PMA (0.05 $\mu\text{g}/\text{ml}$) and ionomycin (0.5 $\mu\text{g}/\text{ml}$) for 4 h. Subsequently, the cells were incubated for a further 2 h in the presence of 2 μM monensin. After washing and surface labeling with PE-conjugated anti-CD8, cells were fixed in PBS containing 2% paraformaldehyde. Thereafter, cells were permeabilized with saponine (0.1%) and unspecific binding to cytoplasmic proteins was blocked with 1:16 diluted normal rat serum. Intracellular cytokines were then stained with FITC-conjugated anti-IFN- γ or FITC-conjugated anti-TNF/LT- α and saponine was removed by washing with buffer solution. Multiparameter analysis was performed with a FACScan[®] using logarithmic scales. Viable cells were gated by forward and side scatter of light.

Statistics. Data are presented as means \pm SD unless stated otherwise. Comparisons were made using the two-tailed unpaired Student's *t* test, the analysis of variance (ANOVA), and the Scheffe's post hoc procedure as appropriate. A *P* value of <0.05 was regarded as significant.

Results

Lethal Pancytopenia Caused by Virus-specific CD8⁺ T Cells in Chronic LCMV Infection of P^{0/0} Mice. The initial CBCs of uninfected P^{0/0} and wt C57BL/6 mice kept under SPF conditions were comparable (Fig. 1). After infection with LCMV, wt C57BL/6 mice showed a moderate, but reversible depression of the CBCs. Neutrophils were lowest on day 3 and reticulocytes on days 9–12 after infection. The transient reduction of platelets and RBCs in C57BL/6 mice was very mild and mainly due to repetitive blood

sampling (Fig. 1 A). In contrast, LCMV-infected P^{0/0} mice exhibited an abrupt and continuous stop of reticulocyte production starting from day 5 post infection (p.i.), the RBC and the thrombocyte count progressively dropped within 14 d, and the neutrophil count remained below 1,000/ μl after day 3. Death ensued between day 14 and 24 p.i. To assess the respective role of CD8⁺ and/or CD4⁺ T cells, thymectomized P^{0/0} mice were treated with either a rat mAb specific for CD4 (YTS 191.1) or a rat anti-mouse CD8 (YTS 169.4) on days -3 and -1 before infection with LCMV (Fig. 1 B). CD8-depleted P^{0/0} mice showed an identical time course of the altered CBCs as compared with CD8-depleted wt C57BL/6 mice (not shown). Compared with untreated LCMV-infected C57BL/6 mice, reticulocytes recovered 4 d earlier and numerically to a lesser extent in CD8-depleted P^{0/0} mice (Fig. 1, A and B). The kinetics of the transient decrease of the thrombocytes and the neutrophils was comparable between CD8-depleted P^{0/0} and untreated C57BL/6 mice, except for a slightly higher neutrophil count after day 10. This difference was probably due to the increased viral load in the CD8-depleted P^{0/0} mice that become LCMV carriers, whereas untreated C57BL/6 mice have cleared LCMV on day 10 (not shown). In contrast, anti-CD4-treated P^{0/0} mice had succumbed similarly to untreated P^{0/0} mice between 14 and 24 d after LCMV infection, due to the severely depressed CBCs (Fig. 1 B). In addition to early induced IFN- α/β (15), these results implicate that LCMV-specific CD8⁺

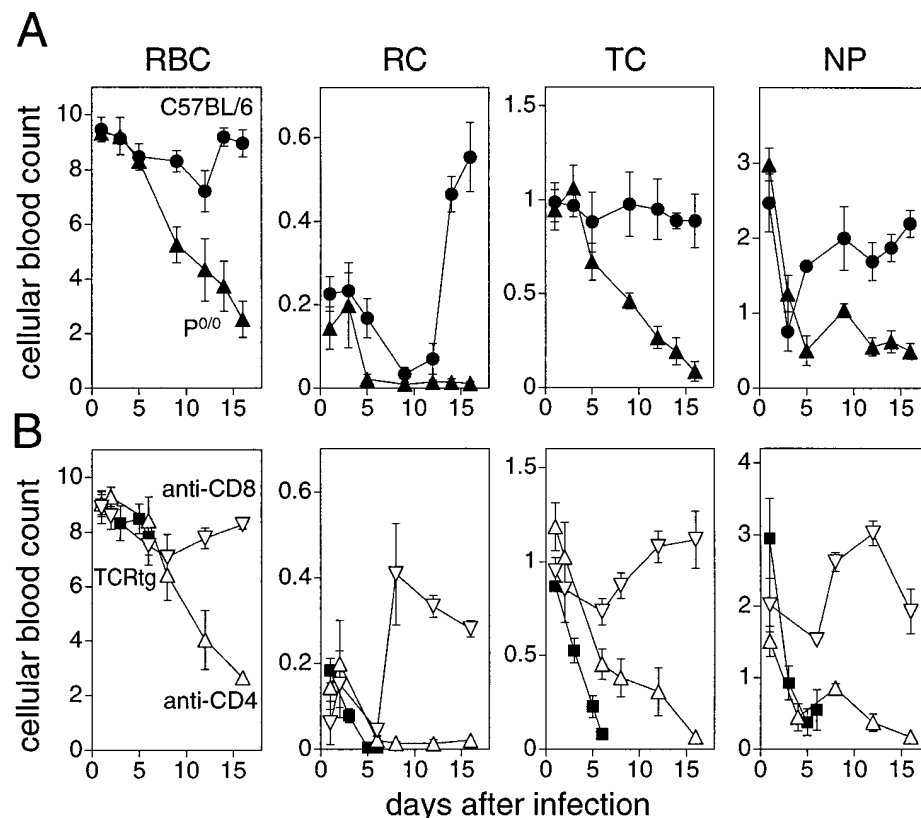


Figure 1. Kinetics of peripheral blood values after infection with LCMV ($10^9/\text{ml}$ RBCs, $10^9/\text{ml}$ reticulocytes [RC], $10^6/\text{ml}$ thrombocytes [TC], $10^6/\text{ml}$ neutrophils [NP]). (A) C57BL/6 mice (●) or P^{0/0} mice (▲) were infected intravenously with LCMV (2×10^2 PFU). Blood was collected from the retroorbital plexus of individual mice at the indicated time points. CBCs were quantified in a hemocytometer and neutrophils were determined microscopically from blood smears. (B) TCR-tg P^{0/0} (■) or thymectomized P^{0/0} mice treated with either anti-CD4 (△) or anti-CD8 (▽) before LCMV infection. The data represent mean \pm SD of four mice per group.

Table 1. Kinetics of BM Cytology of C57BL/6, P^{0/0}, and P^{0/0} × TCR Mice Infected with LCMV

Genotype	Days* after infection	Cell type (%) [§]						
		Megakaryocyte [‡]	Erythroblast	Blasts promyelocyte	Myelocyte metamyelocyte band	Polymorph	Monocyte	Lymphocyte
P ^{0/0}	Uninfected	12–24	35.5 ± 1.0	9.5 ± 1.8	36.5 ± 2.8	5.0 ± 1.5	0.5 ± 0.3	13.0 ± 1.4
C57BL/6	Day 6	6–10	9.5 ± 0.7	27.5 ± 1.4	31.5 ± 1.4	9.5 ± 2.0	5.5 ± 0.8	16.5 ± 2.6
P ^{0/0}		6–12	11.5 ± 0.4	28.5 ± 1.4	27.0 ± 1.8	10.0 ± 2.0	3.0 ± 0.5	20.0 ± 1.3
P ^{0/0} × TCR		4–8	4.0 ± 0.2	27.0 ± 1.3	32.0 ± 1.1	7.0 ± 0.8	3.5 ± 1.5	26.5 ± 2.8
C57BL/6	Day 8	6–10	4.5 ± 0.6	23.0 ± 2.0	37.5 ± 0.8	18.0 ± 1.0	6.0 ± 1.0	11.0 ± 2.3
P ^{0/0}		5–10	7.0 ± 0.3	40.5 ± 2.8	29.0 ± 2.0	3.0 ± 0.1	6.5 ± 0.5	14.0 ± 1.8
P ^{0/0} × TCR		0	2.5 ± 0.4	31.5 ± 3.3	8.0 ± 0.3	1.0 ± 0.3	9.5 ± 4.5	47.5 ± 2.0
C57BL/6	Day 14	8–14	22.0 ± 1.5	16.5 ± 0.8	20.5 ± 2.2	31.0 ± 3.0	1.5 ± 0.8	9.0 ± 0.8
P ^{0/0}		0–3	2.0 ± 0.5	10.0 ± 1.0	28.5 ± 9.2	5.0 ± 1.0	24.0 ± 1.5	29.5 ± 0.3

*Mice (8–12 wk) of different genotypes (three mice per group) were infected with LCMV (2×10^2 PFU). At the time points indicated, BM smears were stained with May-Grünwald/Giemsa, chloracetate esterase, α -naphthyl butyrate esterase, and Sudan black B. Differential counts were obtained microscopically by counting 200 or more cells.

[‡]Numbers represent megakaryocytes per visual field at a magnification of 80. They were determined semiquantitatively by counting at least four visual fields.

[§]Data are means \pm SD of the relative number of total cells per lineage. Eosinophils were included in granulocyte counts.

^{||}P^{0/0} × TCR mice had all died by day 14.

T cells contribute to transient BM suppression also in wt C57BL/6 mice during the later phase of LCMV-infection. The predominant role of LCMV-specific CD8⁺ T cells causing pancytopenia in P^{0/0} mice was further analyzed by infecting P^{0/0} mice expressing a tg TCR specific for the glycoprotein peptide aa33–41 derived from LCMV-GP (P^{0/0} × TCR). In naive P^{0/0} × TCR mice, the proportion of CD8⁺ spleen cells expressing the tg TCR is \sim 50%, and 88% of T cells in the blood periphery are positive for the tg TCR 9 d after LCMV infection (21). As shown in Fig. 1 B, in the presence of an increased frequency of LCMV-specific CD8⁺ T cells in P^{0/0} × TCR mice, the CBCs diminished very rapidly, and within 6–10 d irreversible pancytopenia caused death of infected mice. These TCR-tg mice (V α 2/V β 8.1) allowed us to follow directly the kinetics of LCMV-specific lymphocytes infiltrating and damaging the BM in response to viral replication.

BM Analysis of P^{0/0} Mice after Infection with LCMV in the Presence or Absence of CD4⁺ and CD8⁺ T Cells. To address the question of whether pancytopenia in LCMV-infected P^{0/0} mice reflected consumption or destruction of blood cells rather than suppression of BM function, the different BM compartments (i.e., pluripotent, lineage-committed, and morphologically defined) were studied at several time points after infection. Femoral cellularity in P^{0/0} mice had dropped to $29 \pm 12\%$ of baseline on day 14 and in P^{0/0} × TCR mice to $42 \pm 10\%$ on day 8, whereas in C57BL/6 mice minimal values of $86 \pm 15\%$ were observed 6–8 d after LCMV infection. Serial cytological analysis of BM

preparations revealed a complete loss of megakaryocytes and a gradual deficiency of erythroblasts and postmyeloid myeloid cells until day 8 in P^{0/0} × TCR and day 14 in P^{0/0} mice, respectively (Table 1). A gradual relative increase of marrow monocytes and lymphocytes was noted in P^{0/0} and, more vigorously, in P^{0/0} × TCR mice after LCMV infection. Correlating with the morphologically defined compartment, P^{0/0} mice exhibited a progressive decrease of the number of pluripotent CFU-S (Fig. 2 A) and committed progenitors (Fig. 2 B), which reached minimal values shortly before death on day 14. In LCMV-infected wt C57BL/6 mice, a transient reduction of stem cells was also observed, but it was less severe and was close to normal on day 14 after LCMV infection. CD4-depleted P^{0/0} mice showed loss of committed and pluripotent stem cells comparable to untreated P^{0/0} mice, whereas CD8-depleted P^{0/0} mice had >10 -fold higher numbers of blood cell progenitors after 14 d of LCMV-infection (Fig. 2). Thus, CD8⁺, but not CD4⁺, T cells altered peripheral blood values of LCMV-infected P^{0/0} mice by drastically reducing the frequency of the pluripotent and the lineage-committed stem cells.

Role of Immunopathology versus Autoreactivity in AA of LCMV-infected P^{0/0} Mice. Infiltration of virus-specific T cells into the BM, replication kinetics of LCMV, and type of BM cells infected with LCMV were assessed in P^{0/0} and P^{0/0} × TCR mice at various time points after infection. Both strains of P^{0/0} (TCR tg and TCR non-tg) showed a similar kinetics of LCMV replication in the BM and a comparable plateau of persisting viral load in the range of

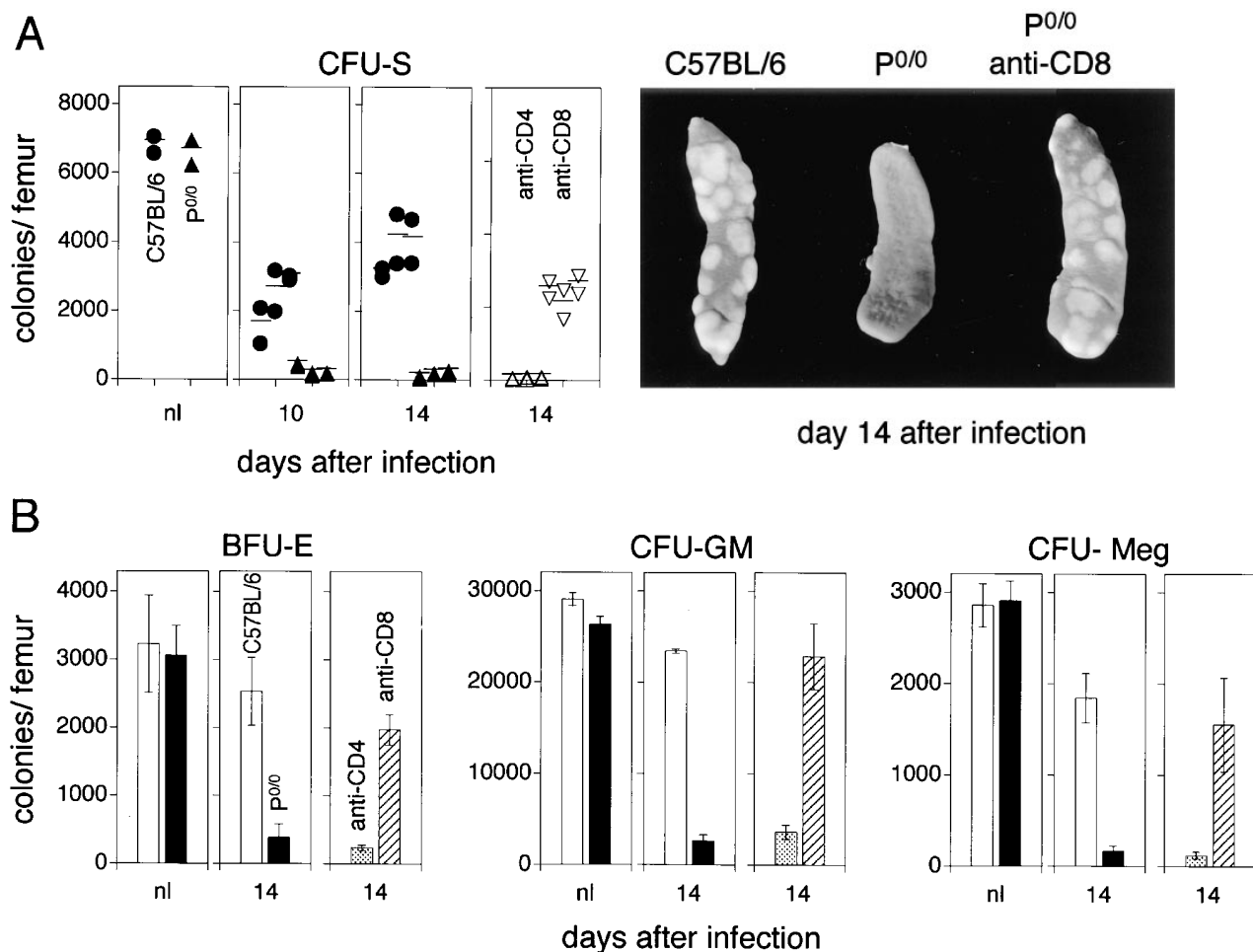


Figure 2. Number of stem cells in the BM after LCMV infection. (A) To determine the pluripotent hematopoietic progenitors (CFU-S), 10^5 syngeneic BM cells of normal or infected C57BL/6 mice (●), P^{0/0} (▲), or thymectomized P^{0/0} mice treated with either anti-CD4 (△) or anti-CD8 (▽) donor mice were injected intravenously into lethally irradiated LCMV-immune recipient C57BL/6 mice (H-2^b). CFU-S were determined 12 d later on the surface of the spleen (photograph). Each dot shows the number of colonies of an individual recipient. The horizontal lines represent the mean number of colonies per femur transferred from one individual donor mouse. The mean CFU-S of three individual donor mice per group are shown. (B) Lineage-committed precursors in C57BL/6 mice (white columns) or P^{0/0} (black columns) or thymectomized P^{0/0} mice treated with either anti-CD4 (dotted columns) or anti-CD8 (hatched columns). Results are presented as the mean number (\pm SD) of BFU-E, CFU-GM, or CFU-Meg for duplicate methylcellulose cultures of total BM cells per femur. Pooled data from two independent experiments with two individual mice per group are shown.

10^3 – 10^4 PFU/ 10^7 BM cells after day 6 of LCMV infection (Fig. 3 A). In contrast, viral titers in wt C57BL/6 mice did not exceed 10^2 PFU/ 10^7 nucleated BM cells and were below detection levels already on day 8 p.i. Concomitant expansion of polyclonal CD8⁺ T cells and T cells expressing the TCR for gp33 presented on H-2^b were followed flow cytometrically by staining BM cells with a CD8- and a TCR-V α 2-specific mAb (Fig. 3 B). By day 2 after LCMV infection, the frequency of CD8⁺ T cells expressing the V α 2 segment of the TCR was \sim 2% of all nucleated BM cells and reached maximal levels 6 d p.i. in P^{0/0} \times TCR mice. In P^{0/0} mice, BM infiltration with polyclonal CD8⁺ T cells was less vigorous, but their proportion persisted above 20% of BM cells until 14 d after LCMV infection. Morphologically defined hematopoietic cells (according to Table 1) infected with LCMV were detected by staining BM smears with an LCMV-specific mAb (15) and N418,

an antibody detecting CD11c on dendritic cells (Fig. 3 C). Although LCMV Ag was expressed in great amounts in CD11c-positive APCs and stromal BM cells, LCMV did not replicate to a detectable extent in hematopoietic cells in C57BL/6, P^{0/0}, and P^{0/0} \times TCR mice at any time point of infection. Additionally, staining with the same mAb of picked colonies of BFU-E, CFU-GM, and CFU-Meg of infected P^{0/0} mice did not reveal replication of LCMV in early hematopoietic progenitors (data not shown).

To study whether blood cell precursors in the BM shared antigenic determinants with LCMV and cross-reactivity to self-Ags was involved in AA of LCMV-infected P^{0/0} and P^{0/0} \times TCR mice, an experimental approach was chosen that has been described previously (21). TCR-tg T cells were activated by infecting P^{0/0} \times TCR mice intravenously with 2×10^6 PFU of vacc-LCMV-GP. After 6 d, 5×10^6 spleen cells were adoptively transferred into sex-

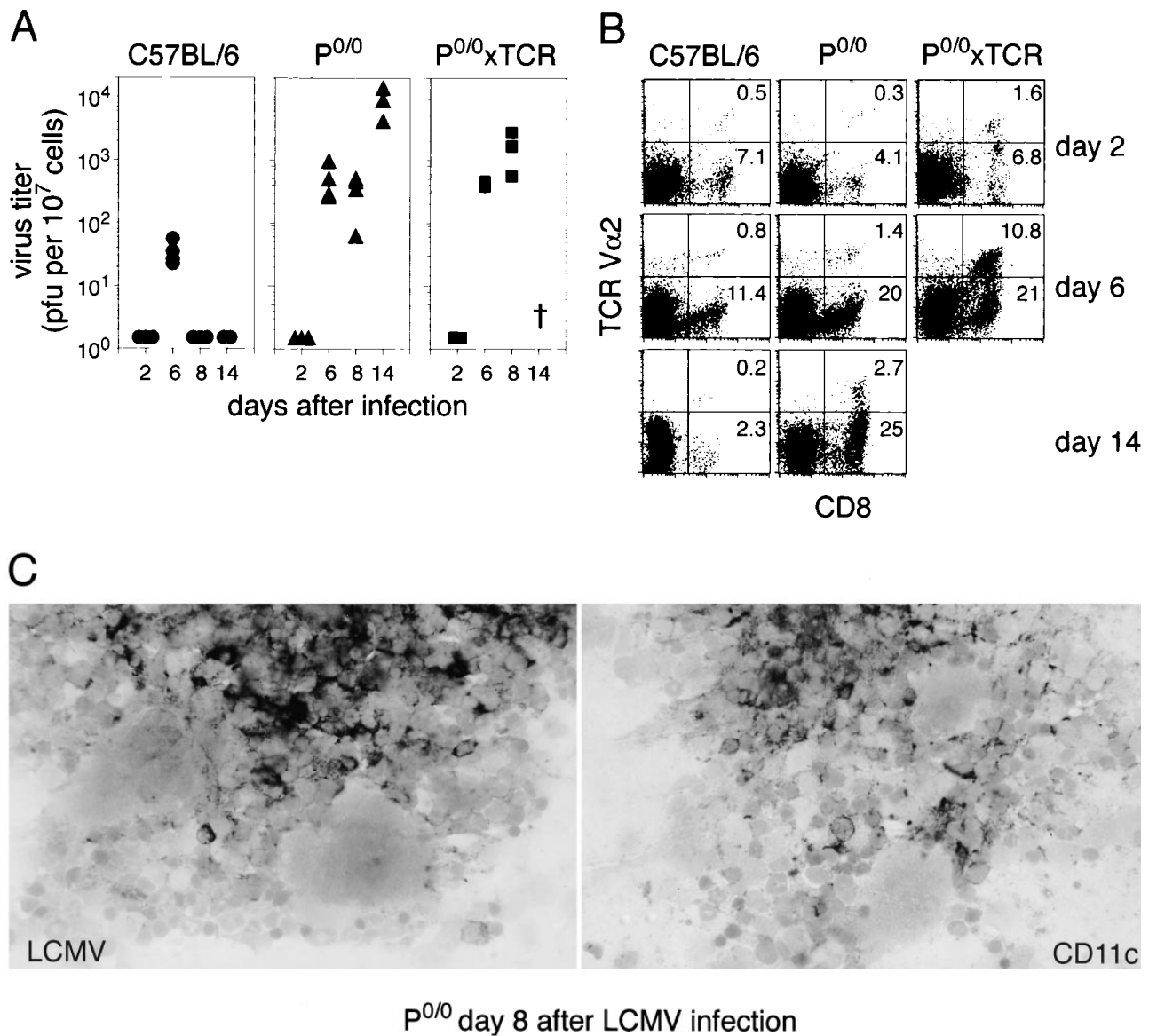


Figure 3. LCMV titers and infection of dendritic cells correlating with expansion of T cells in the BM. (A) LCMV titers were determined in a focusing assay and are given as PFU per 10^7 nucleated BM cells. Data points are values for three individual mice. (B) tg CD8⁺ T cells expressing a TCR specific for the gp peptide aa33-41 derived from LCMV presented on H-2D^b were detected in the CD8⁺/TCR-Vα2⁺ compartment by FACS[®] analysis. Lower right quadrant, Expansion of endogenous T cells in TCR tg P^{0/0} (P^{0/0} × TCR) and CD8⁺ T cells of non-tg P^{0/0} or C57BL/6 mice. Populations represent frequencies of total nucleated BM cells and dot plots are representative of three mice. (C) Immunocytochemical staining of BM smears with an LCMV (VL4)- and CD11c (N418)-specific mAb. The respective cells expressing either LCMV or CD11c appear black.

matched, syngeneic tg mice expressing LCMV-GP in their pancreas. Applying this protocol, gp33-specific tg T cells were strongly activated, but vaccinia virus was efficiently eliminated before the transfer of T cells because in the absence of perforin, the ability to control vaccinia virus is retained (35). This allowed us to circumvent cotransfer of virus leading subsequently to uncontrolled viral replication in recipient mice, as seen in LCMV-infected P^{0/0} and P^{0/0} × TCR mice. To keep the transferred cells in an activated state, the recipients were infected intravenously with 2×10^6 PFU vacc-LCMV-GP. All recipients receiving P^{0/0} × TCR spleen cells developed insulinitis, i.e., extensive infiltra-

tion of CD8⁺ T cells into the pancreatic islets expressing the LCMV-GP transgene was found histologically (21). In contrast, no abnormalities of the CBCs were detected 10 d and later after adoptive transfer of the tg T cells into the same recipient mice (Table 2). Using the same experimental setup, a normal CBC was also obtained after transfer of activated TCR-tg T cells into syngeneic C57BL/6 mice that do not express the LCMV-GP transgene in their pancreas. Collectively, these findings made a direct, cognate cell to cell interaction between virus-specific CD8⁺ T cells and hematopoietic progenitors expressing either LCMV peptides or cross-reactive self-epitopes on H-2^b, subse-

Table 2. Peripheral Blood Values of LCMV-GP *tg* Mice after Adoptive Transfer with LCMV-GP-specific T Cells

Donor T cells*	Recipient [‡]	Infection of recipient	Infiltration of islets	CBC [§] of recipients (10 d after adoptive transfer)		
				Reticulocytes	Platelets	Neutrophils
None	No transgene	None	–	215 ± 10	953 ± 110	4.5 ± 0.2
None	No transgene	vacc-LCMV-GP	–	210 ± 28	1,021 ± 92	3.8 ± 0.1
P ^{0/0} × TCR	LCMV-GP	vacc-LCMV-GP	++++	221 ± 15	1,271 ± 145	4.0 ± 0.4
P ^{0/0} × TCR	No transgene	vacc-LCMV-GP	–	229 ± 25	998 ± 84	4.7 ± 0.3

*LCMV-GP-specific T cells were activated by infecting P^{0/0} × TCR mice with 2 × 10⁶ PFU vacc-LCMV-GP intravenously. 6 d later, 5 × 10⁶ spleen cells were transferred into syngeneic recipients (H-2^b).

[‡]Recipient mice expressed LCMV-GP as a transgene under the rat insulin promoter in the β cells of the pancreatic islets (47). To keep the transferred cells activated, recipient mice were infected intravenously with 2 × 10⁶ PFU vacc-LCMV-GP after transfer. Pancreatic islets were analyzed histologically and have been described previously (21).

[§]CBCs were quantified in a hemocytometer, and neutrophils were determined microscopically from blood smears. Values are × 10⁶/ml.

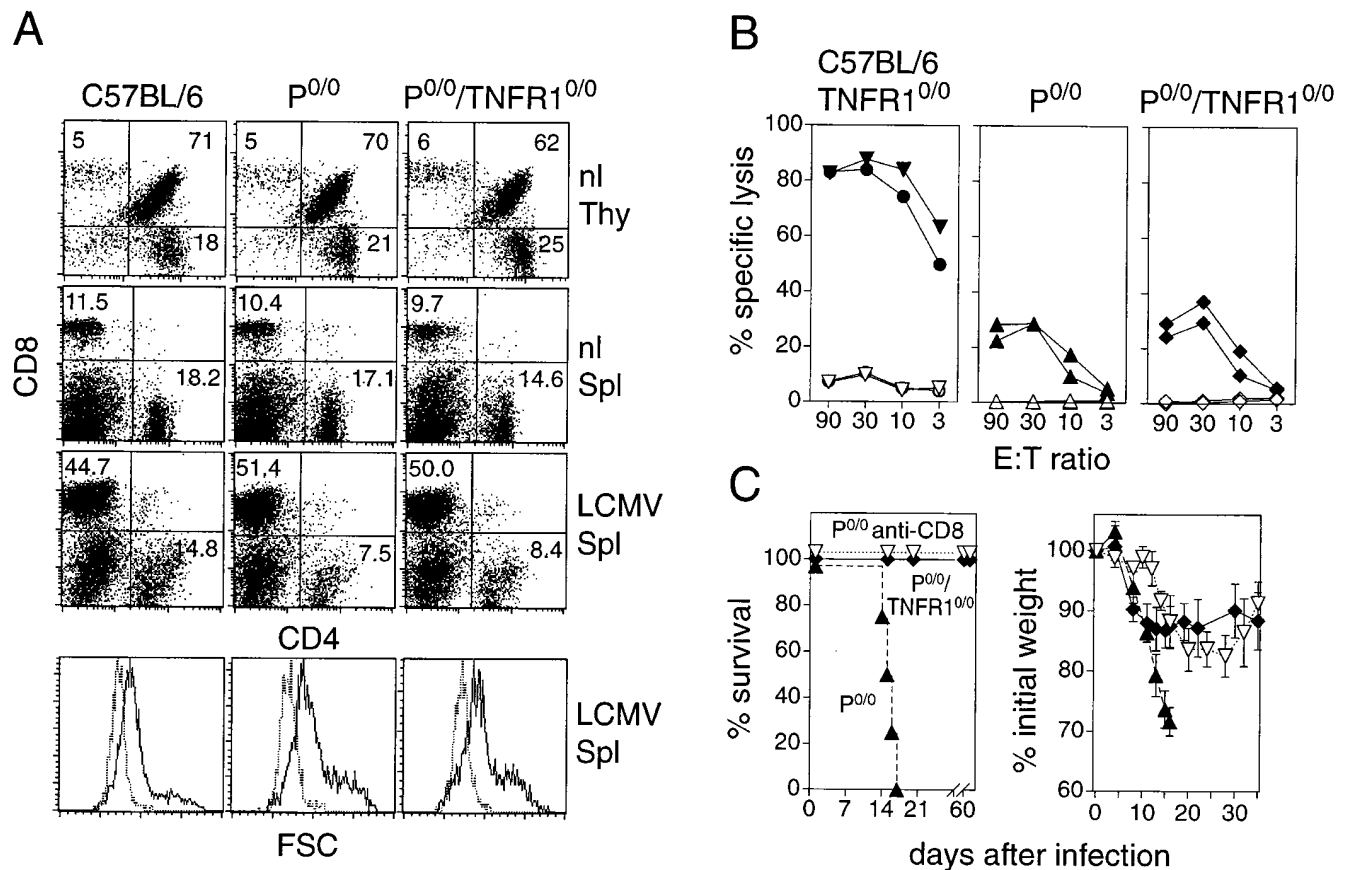


Figure 4. Comparison of different lymphocyte populations of uninfected (*nl*) C57BL/6, P^{0/0} and P^{0/0}/TNFR1^{0/0} mice, and consequences of LCMV infection in vivo. (A) Normal development of CD4⁺ and CD8⁺ T cell compartments in thymus (*Thy*) and spleen (*Spl*). Activation and expansion of spleen cells was compared between different mouse strains 8 d after infection with LCMV (200 PFU). Blast formation of activated T cells was demonstrated by comparing forward scatter (*FSC*) of CD8⁺ T cells from LCMV-infected (*solid line*) mice with uninfected (*dotted line*) mice. (B) LCMV-specific CTL activity measured on lymphohematopoietic target cells after a primary infection with LCMV. RMA lymphoma cells were either uninfected (*open symbols*) or labeled with peptide aa33-41 of LCMV-GP (●, C57BL/6; ▼, TNFR1^{0/0} mice) presented by H-2D^b. Lytic activity was measured in a 5-h⁵¹Cr-release assay; spontaneous release < 15%. (C) Overall health status after infection with LCMV as assessed by survival and loss of body weight. P^{0/0} mice (▲, *dashed lines*) were either thymectomized and depleted of CD8⁺ T cells (▽, *dotted lines*) or lacked the expression of TNFR1 (P^{0/0}/TNFR1^{0/0} ◆, *solid lines*).

quently leading to destruction of stem cells and development of AA, very unlikely.

Effects of LCMV Infection on Survival, Viral Replication, and T Cell Response in $P^{0/0}$ Mice that Lack TNFR1 Expression. To test a possible T cell-dependent damaging effect of TNF/LT- α in AA of LCMV-infected $P^{0/0}$ mice, $P^{0/0}$ mice were crossed into TNFR1 $^{0/0}$ mice. These mutants exhibit normal CTL induction and effector functions against LCMV (28). Lymphocyte subpopulations in the thymus and the spleen in these double knockouts ($P^{0/0}$ /TNFR1 $^{0/0}$) were comparable to wt C57BL/6 mice, i.e., the concurrent deficiency of perforin and TNFR1 in individual mice did not alter the proportion of the two T cell compartments in these lymphoid organs (Fig. 4 A, *top*). Activation and expansion of T cells in the spleen were followed by FACS[®] analysis 8 d after infection with LCMV (Fig. 4 A, *bottom*). Both $P^{0/0}$ and $P^{0/0}$ /TNFR1 $^{0/0}$ mice showed a similar increase in CD8⁺ T cells by a factor of ~ 5 and the typical inversion of the CD4⁺/CD8⁺ ratio from 1.5 of uninfected to 0.15 of infected individuals on day 8 after infection. In parallel, expanding CD8⁺ T cells in the spleen were similarly activated in both mutant mouse strains, as demonstrated by the increased forward light scatter of CD8⁺ T cells. (Note the significantly higher proportion of large blasts in $P^{0/0}$ and $P^{0/0}$ /TNFR1 $^{0/0}$ mice when compared with C57BL/6 mice [Fig. 4 A, *bottom*].) The cytolytic effector function of LCMV-induced CTLs was then assessed in an in vitro ⁵¹Cr-release assay 8 d after infection with LCMV (Fig. 4 B). Spleen cells from $P^{0/0}$ and $P^{0/0}$ /TNFR1 $^{0/0}$ mice did not lyse peptide-labeled MC57G fibrosarcoma (H-2^b) targets (not shown), whereas residual virus-specific, Fas/CD95-mediated cytolytic activity was comparably detected on gp33-labeled RMA lymphoma cells (H-2^b) in both mouse strains. By comparison, both parental strains (C57BL/6 and TNFR1 $^{0/0}$) exhibited an equal cytolytic activity on gp33-

labeled fibroblast (not shown) and lymphoma targets (Fig. 4 B). Infection with LCMV was lethal in age- and sex-matched $P^{0/0}$ mice by day 21 after infection (Fig. 4 C, *left*). In contrast, $P^{0/0}$ /TNFR1 $^{0/0}$ mice survived LCMV infection and demonstrated a loss of initial body weight and subsequent runting disease comparable to thymectomized, CD8-depleted $P^{0/0}$ mice (Fig. 4 C, *right*). The kinetics of viral replication was next examined in various solid organs and hematopoietic tissues after different time points of LCMV infection (Table 3). The increase in viral load was comparable between $P^{0/0}$ /TNFR1 $^{0/0}$ and $P^{0/0}$ mice, and maximal viral titers had reached similar values in all organs tested already by day 8, reflecting an unaltered susceptibility to LCMV replication in $P^{0/0}$ mice deficient in TNFR1 as opposed to $P^{0/0}$ control mice. In contrast, wt C57BL/6 and TNFR1 $^{0/0}$ mice had cleared LCMV by day 14 after infection below detection levels. Surviving $P^{0/0}$ /TNFR1 $^{0/0}$ mice remained persistently infected with LCMV and exhibited a mild decrease in viral titers in most organs on day 90 after infection. These findings indicate that the deficient signaling via TNFR1 provides LCMV-infected $P^{0/0}$ mice with a selective advantage over parental $P^{0/0}$ mice; additional lack of TNF function prevents death and leads to a life-long viral persistence, despite quantitatively and qualitatively comparable T cell responses and viral replication kinetics after infection with LCMV.

CBCs and Functional BM Compartments after LCMV Infection of Mice Devoid of Perforin and TNFR1. Because $P^{0/0}$ /TNFR1 $^{0/0}$ mice survived LCMV infection, we anticipated their CBCs to differ significantly from that of $P^{0/0}$ mice during LCMV infection. Surprisingly, both mutants exhibited a similar decline of the RBC and platelet count during the first 14 d and both abruptly ceased to produce reticulocytes on day 5 after infection with LCMV (Fig. 5 A). Between days 14 and 30 after LCMV infection, however, $P^{0/0}$ /

Table 3. Virus Titers of C57BL/6, $P^{0/0}$, and $P^{0/0}$ /TNFR1 $^{0/0}$ Mutants in Different Organs after Various Time Points of LCMV Infection

Genotype	Days after infection*	Virus titer per ml or gram organ [†]					
		Blood	Bone marrow	Spleen	Thymus	Liver	Kidney
		<i>PFU</i>	<i>PFU</i>	<i>PFU</i>	<i>PFU</i>	<i>PFU</i>	<i>PFU</i>
C57BL/6	8	1.0×10^2	<10	5.2×10^3	3.0×10^3	<100	<100
	14	<50	<10	<75	<90	<100	<100
$P^{0/0}$	8	3.4×10^4	7.4×10^3	1.8×10^7	7.8×10^5	1.9×10^6	4.5×10^5
	14	2.2×10^4	6.7×10^3	6.5×10^7	2.8×10^6	6.8×10^7	2.1×10^6
$P^{0/0}$ /TNFR1 $^{0/0}$	8	6.1×10^4	6.7×10^3	2.4×10^7	9.7×10^5	1.3×10^6	3.1×10^5
	14	6.3×10^4	6.4×10^3	6.0×10^7	8.6×10^6	5.6×10^7	3.1×10^7
	40	3.0×10^3	3.0×10^3	9.0×10^5	2.1×10^5	7.3×10^5	1.1×10^6
	90	3.3×10^3	4.0×10^2	4.9×10^6	5.0×10^5	6.8×10^4	3.3×10^5

*Mice were infected with a low dose of LCMV (2×10^2 PFU); organs were removed at the indicated time points after infection.

[†]Viral titers of the various organs were determined individually in a focus-forming assay and are given as PFU per gram of tissue for solid organs. Blood titers are shown as PFU/ml and BM titers as PFU/ 10^7 nucleated BM cells. Data represent means of three to four mice. SD varied between 0.01 and 0.4 log₁₀.

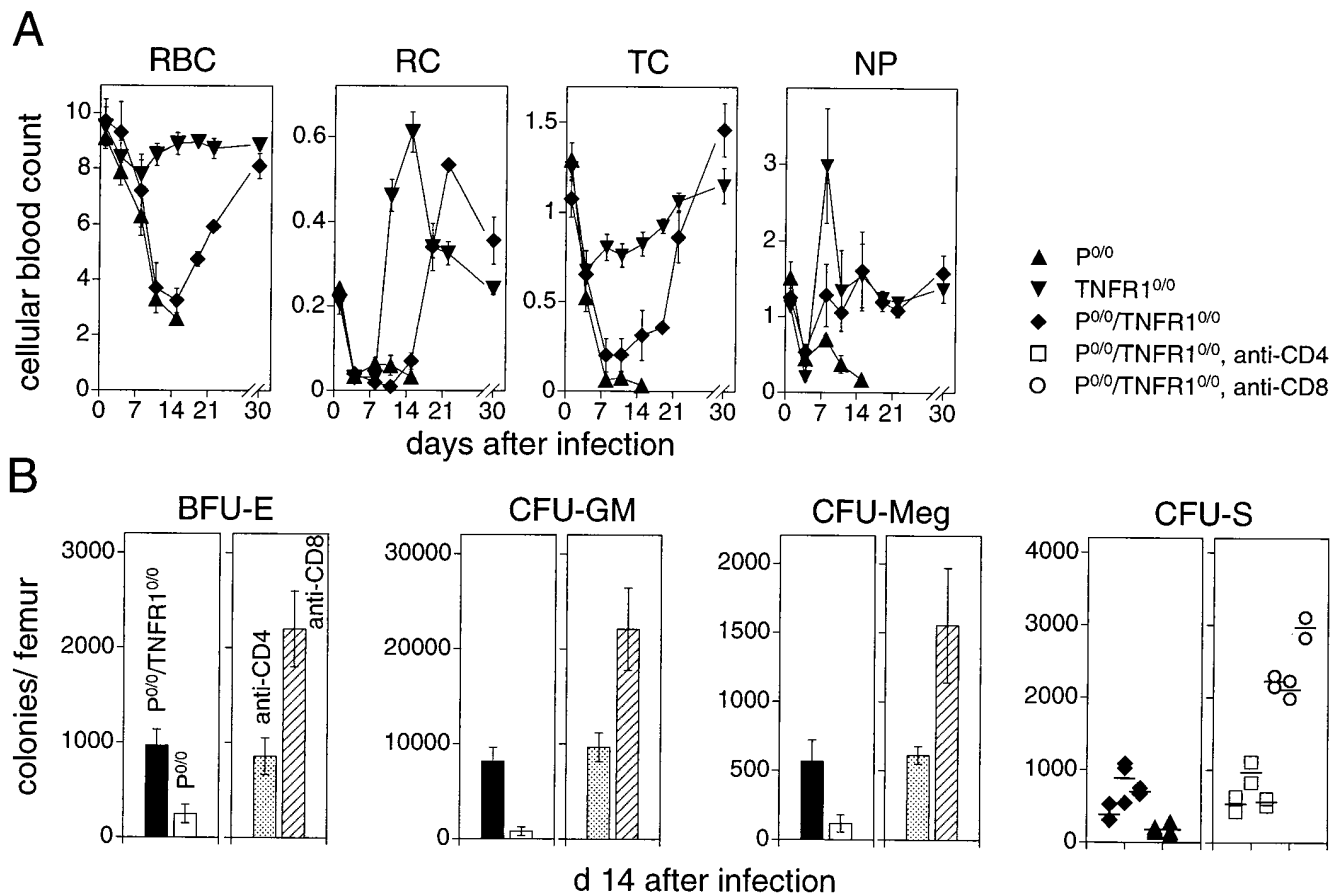


Figure 5. Kinetics of CBCs and numbers of lineage-committed and pluripotent progenitors in the BM depending on expression of TNFR1 in persistent LCMV infection. (A) 10^9 /ml RBCs, 10^9 /ml reticulocytes [RC], 10^9 /ml thrombocytes [TC], 10^6 /ml neutrophils [NP]. Blood was collected from the retrobulbar plexus of individual TNFR1^{0/0} (▼), P^{0/0} (▲), and P^{0/0}/TNFR1^{0/0} (◆) mice at the indicated time points (four mice per group). CBCs were quantified in a hemocytometer and neutrophils were determined microscopically from blood smears. (B) Lineage-committed precursors after LCMV infection in P^{0/0}/TNFR1^{0/0} (black columns) or P^{0/0} (white columns) mice and thymectomized P^{0/0}/TNFR1^{0/0} mice treated with either anti-CD4 (dotted columns) or anti-CD8 (hatched columns). Data show the mean number (\pm SD) of BFU-E, CFU-GM, or CFU-Meg for duplicate methylcellulose cultures of total BM cells per femur on day 14. The pluripotent hematopoietic progenitors (CFU-S) were determined as described in Materials and Methods on day 14 of infection. CFU-S in the spleens of P^{0/0}/TNFR1^{0/0} mice (◆) or P^{0/0} (▲) and thymectomized P^{0/0}/TNFR1^{0/0} mice treated with either anti-CD4 (□) or anti-CD8 (○) were quantified in lethally irradiated LCMV-immune recipient C57BL/6 mice (H-2^b). Each dot shows the number of colonies of an individual recipient. The horizontal lines represent the mean number of colonies per femur transferred from one individual donor mouse.

TNFR1^{0/0} mice showed a vigorous regeneration of these blood cells, whereas P^{0/0} mice failed to increase their CBCs. The most apparent difference between LCMV-infected P^{0/0} and P^{0/0}/TNFR1^{0/0} mice was observed in the number of peripheral PMNs, which did not drop below a value of $\sim 1,000/\mu\text{l}$ in P^{0/0}/TNFR1^{0/0} mice, whereas in P^{0/0} mice, generally $< 500/\mu\text{l}$ neutrophils were counted after day 8 of LCMV infection. As expected from earlier data (28), the CBCs of LCMV-infected, parental TNFR1^{0/0} mice (Fig. 5 A) showed no significant difference when compared with LCMV-infected C57BL/6 mice (Fig. 1 A).

To address the question of whether the transient depression of the CBCs was also mediated by CD8⁺ T cells, thymectomized, CD4- and CD8-depleted individuals were included in the experiments designed to determine the number of progenitors in the BM of LCMV-infected P^{0/0}/TNFR1^{0/0} mice. On day 8 after LCMV infection, the number of pluripotent and committed stem cells did not

differ significantly between P^{0/0}/TNFR1^{0/0} and parental P^{0/0} mice (not shown). In contrast, on day 14 p.i., when the beginning of the reticulocyte crisis and point of return of the CBC was noted, hematopoietic progenitors were 4–10-fold increased in P^{0/0}/TNFR1^{0/0} mice when compared with P^{0/0} mice at the same time point (Fig. 5 B). Thus, besides TNF/LT- α , an additional CD8⁺ T cell-mediated activity was apparently involved in LCMV-induced AA because the numbers of stem cells in CD8- (but not CD4-) depleted P^{0/0}/TNFR1^{0/0} mice increased after LCMV infection and were then comparable to uninfected P^{0/0}/TNFR1^{0/0} mice (Fig. 5 B).

IFN- γ Production by LCMV-specific CD8⁺ T Cells in P^{0/0} and P^{0/0}/TNFR1^{0/0} Mice. In addition to TNF/LT- α , T cell-dependent IFN- γ is known to inhibit hematopoietic colony formation in vitro (36). We therefore evaluated whether CD8⁺ T cells in LCMV-infected mutants produced IFN- γ , causing residual blood disease in P^{0/0}/

TNFR1^{0/0} mice. Serum samples of LCMV-infected P^{0/0} and P^{0/0}/TNFR1^{0/0} mice were serially analyzed for the presence of IFN- γ and TNF with a cytokine-specific ELISA, detecting TNF and LT- α . From days 4 to 10 after LCMV infection, increasing amounts of these cytokines were measured in the serum with maximal values of 100 U/ml of IFN- γ and 60 ng/ml of TNF/LT- α on day 10. The serum concentrations of the cytokines did not differ significantly between P^{0/0} and P^{0/0}/TNFR1^{0/0} mice, but both cytokines were below detection limit in LCMV-infected C57BL/6 control mice during the entire study period (not shown). To identify cytokine-producing lymphocytes in vivo, the proportion of MACS[®]-enriched CD8⁺ spleen cells, expressing cytokines in the cytoplasm, were measured by FACS[®] analysis (Fig. 6 A). Before LCMV infection, background levels of IFN- γ -positive CD8⁺ T cells were comparable in all mouse strains but 8 d later, a similar increase of IFN- γ -expressing CD8⁺ T cells was detected in P^{0/0} and P^{0/0}/TNFR1^{0/0} mice, whereas the frequency of these cells was lower in infected C57BL/6 mice. Intracellular production of IFN- γ by bulk CD8⁺ T cells in vivo was LCMV-GP specific, i.e., on day 8 after infection, CD8⁺ spleen cells of LCMV-infected mutant and wt mice secreted similar amounts of soluble IFN- γ when restimulated in vitro with irradiated APCs pulsed with gp33 in the presence or absence of IL-2 (Fig. 6 B). However, in contrast to C57BL/6 mice, gp33-specific, IFN- γ secreting CD8⁺ T cells had disappeared in P^{0/0} and P^{0/0}/TNFR1^{0/0} mice on day 14 after LCMV infection. Neither cytoplasmic mAb staining for TNF/LT- α nor restimulation in vitro with gp33 or LCMV revealed production of TNF/LT- α by CD8⁺ T cells above the detection limit, indicating that the source of TNF/LT- α was not LCMV-specific CD8⁺ T cells. Thus, induction of cytokine-secreting, CD8⁺ T cell responses by LCMV was unimpaired in P^{0/0} and P^{0/0}/TNFR1^{0/0} mice when compared with wt C57BL/6 mice, but due to the overwhelming replication of LCMV in lympho-hematopoietic and solid tissue in these mutants, LCMV-specific CD8⁺ T cells secreting IFN- γ were eventually exhausted, irrespective of the presence or absence of TNFR1 signaling.

Dominant Role of IFN- γ over TNF/LT- α in Causing LCMV-induced AA. To further dissect the effect of individual cytokines involved in virus-induced AA, LCMV-infected mutants, lacking function of IFN- γ , were studied. Because the perforin and the IFN- γ R gene are both located on the same chromosome, interrupting the IFN- γ -signaling pathway was not readily feasible (i.e., by crossing IFN- γ R^{0/0} mice into P^{0/0} mice), and therefore an IFN- γ -neutralizing sheep anti-mouse IFN- γ antiserum (32) was used. P^{0/0} mice were treated daily from days 5 to 15 after infection with LCMV with 2 \times 10⁴ NU anti-IFN- γ intraperitoneally and control mice were injected with the same volume of normal sheep serum (NSS). P^{0/0} mice treated with anti-IFN- γ survived LCMV infection and became virus carriers similar to NSS- and anti-IFN- γ -treated P^{0/0}/TNFR1^{0/0} mice (not shown), whereas NSS-treated P^{0/0} mice died within the usual time period.

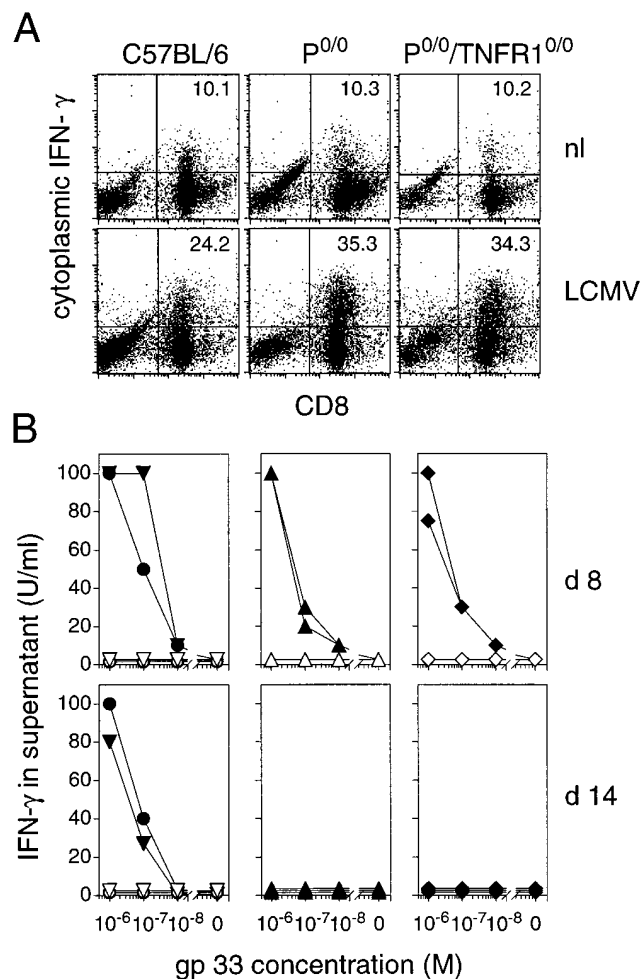


Figure 6. Production of IFN- γ by CD8⁺ T cells, isolated from LCMV-infected C57BL/6 and mutant P^{0/0} or P^{0/0}/TNFR1^{0/0} mice. (A) Cytokine-expressing T cells were identified in vivo in MACS[®]-enriched CD8⁺ spleen cells after stimulation with PMA and ionomycin in vitro. CD8⁺ T cells were isolated from spleens of either uninfected controls (nl) or mice infected 8 d previously with LCMV. The proportion of cells expressing intracellular IFN- γ was measured by FACS[®] analysis; the numbers in dot plots indicate percentages of cells expressing IFN- γ gated for CD8⁺ cells. Lower left quadrants. Cells were 20–25% of purified spleen cells and were mainly CD4⁺ T cells. Plots are representative for three mice per group. (B) Detection of IFN- γ -secreting virus-specific T cells at 8 and 14 d after LCMV infection in parental C57BL/6 (●) and TNFR1^{0/0} (▼) or mutant P^{0/0} (▲) and P^{0/0}/TNFR1^{0/0} (◆) mice. Corresponding uninfected control mice of the same genotype were included in the same experimental settings (open symbols). MACS[®]-enriched CD8⁺ spleen cells of infected wt and mutant mice were restimulated in vitro with irradiated syngeneic APCs coated in threefold serial dilutions with gp33 in the presence of IL-2. After 48 h, IFN- γ was measured in an ELISA; numbers on ordinates represent IFN- γ concentrations in supernatant (U/ml).

The CBCs improved drastically in anti-IFN- γ -treated P^{0/0} mice during the critical time period, starting on day 10 after LCMV infection, when compared with NSS-treated controls (Fig. 7, A and B, left). In LCMV-infected P^{0/0}/TNFR1^{0/0} mice, the effect of daily anti-IFN- γ treatment was more moderate, i.e., the increase of the neutrophil count was only about fourfold when compared with NSS-

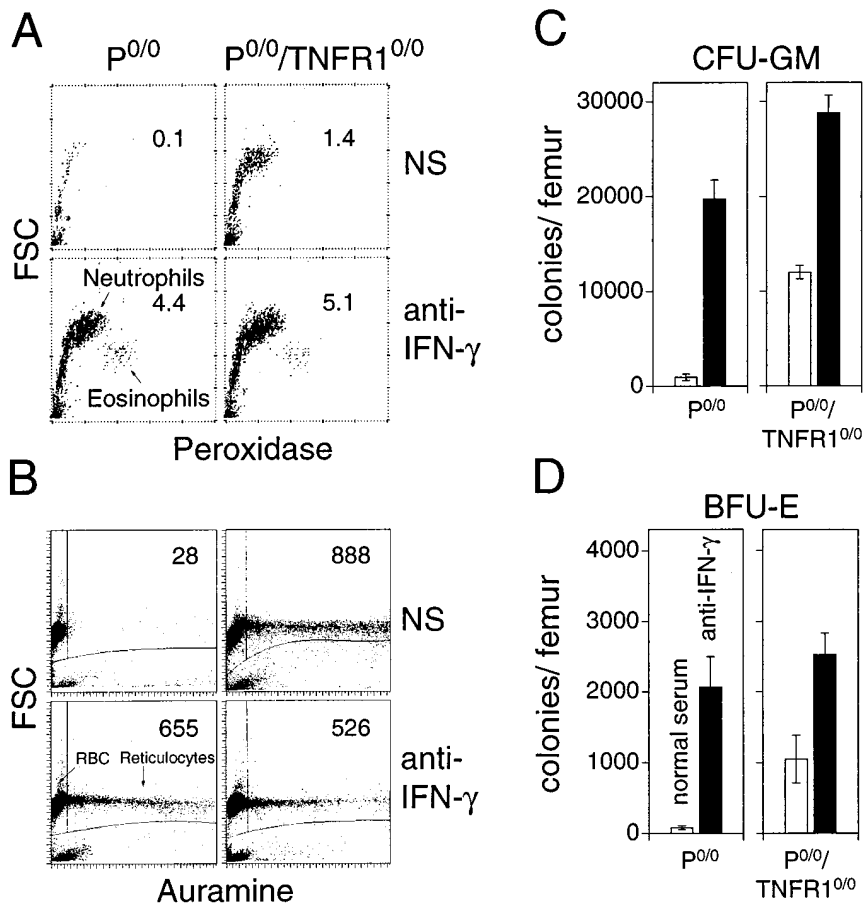


Figure 7. Influence on RBC and neutrophil formation by neutralizing IFN- γ during chronic LCMV infection in $P^{0/0}$ and $P^{0/0}/TNFR1^{0/0}$ mice. From days 5 to 15 after LCMV infection, mice were injected daily with sheep anti-IFN- γ (*anti-IFN- γ*) or sheep normal serum (NS) intraperitoneally. (A) Hemocytogram showing leukocyte counts in $P^{0/0}$ mice treated with normal sheep serum on day 14 after LCMV infection (plot representative for four mice/treatment group). Neutrophils are identified by their positive staining for peroxidase; numbers in plots delineate neutrophils ($\times 10^6/ml$) determined microscopically from blood smears. (B) Circulating reticulocytes quantitated flow cytometrically by unspecific RNA staining with auramine-O. The y-axis shows forward scatter (FSC) and the x-axis shows fluorescence. Cells with a high fluorescence intensity represent young reticulocytes containing high amounts of RNA and are separated from the area of mature RBCs by a vertical line. The horizontal curve separates platelets from RBCs and reticulocytes. Numbers in plots are absolute numbers of reticulocytes in the blood ($\times 10^6/ml$). (C and D) Myeloid and erythroid precursors in the BM of mice treated with sheep normal serum (*open columns*) or sheep anti-IFN- γ (*black columns*) 14 d after LCMV infection. Values show the mean number (\pm SD) for duplicate methylcellulose cultures of total BM cells per femur. Pooled data from three individual mice per group are shown.

treated $P^{0/0}/TNFR1^{0/0}$ mice (Fig. 7 A, right). Because the number of RBCs in anti-IFN- γ -treated $P^{0/0}/TNFR1^{0/0}$ mice decreased only to a mild extent, the regeneration of RBCs on day 14 after LCMV infection was weaker than that of NSS-treated $P^{0/0}/TNFR1^{0/0}$ mice. This is reflected by a less vigorous production of reticulocytes when anti-IFN- γ treatment was given daily to LCMV-infected $P^{0/0}/TNFR1^{0/0}$ mice (Fig. 7 B, right). Moreover, the number of eosinophils of both $P^{0/0}$ and $P^{0/0}/TNFR1^{0/0}$ mice had returned to normal levels 14 d after LCMV infection when the mutants were treated with anti-IFN- γ , but not when treated with NSS (Fig. 7 A, bottom). After neutralizing IFN- γ in LCMV-infected $P^{0/0}$ mice with daily anti-IFN- γ treatment, CFU-GM and BFU-E were 1.5–2-fold higher than in NSS-treated $P^{0/0}/TNFR1^{0/0}$ mice 14 d after infection (Fig. 7, C and D). When both cytokines were blocked during LCMV infection (anti-IFN- γ -treated $P^{0/0}/TNFR1^{0/0}$ mice), committed stem cell frequencies were comparable to CD8 $^{+}$ -depleted $P^{0/0}$ and normal C57BL/6 mice on day 14 after LCMV infection. These findings collectively indicate that the myelosuppressive effect of IFN- γ in chronically infected $P^{0/0}$ mice was much more efficient when compared in the absence of TNF/LT- α function, as analyzed in LCMV-infected $P^{0/0}/TNFR1^{0/0}$ mice.

Discussion

Mechanism of Development and Rescue from Aplastic Anemia

LCMV-infected $P^{0/0}$ mice represent a model for virus-associated AA as they develop a disorder that shares most of the hematologic and immunologic properties of human AA associated with seronegative hepatitis for A-G or other viral infections that are not cytopathic for hematopoietic cells. It manifests as a progressive pancytopenia with uniform depression of the CBC that is lethal for 100% of infected mice. Morphologically, the blood smear shows no abnormalities and analysis of the precursors in the BM reveals drastically reduced numbers of hematopoietic progenitors, including those for erythroid cells (BFU-E), myeloid cells (CFU-GM), megakaryocytes (CFU-Meg), and stem cells (CFU-S 12). Depletion experiments with mAb demonstrate the critical role of CD8 $^{+}$ T cells but not of CD4 $^{+}$ T cells or NK cells, a finding corresponding closely to the immune phenotype found in the BM and blood of patients with AA (37). Acceleration of disease in TCR-tg animals is reminiscent of the association between certain MHC class I alleles and the incidence of AA in some patient populations, which may reflect differences in the TCR repertoire

or precursor frequency being involved in progression to severe disease (10). TNF/LT- α and IFN- γ are the most important inhibitory molecules of hematopoiesis in AA of LCMV-infected P^{0/0} mice, and are also detected in marrow cell preparations from most cases with AA in humans (38–40).

CTL-mediated Immunopathology. AA in LCMV-infected P^{0/0} mice is the consequence of a nonbalanced antiviral immune response caused by a conflict between persisting viral Ag and continuously expanding CD8⁺ T cells in the BM. In the presence of a comparable viral load and similar replication kinetics of LCMV in P^{0/0} and TCR-tg P^{0/0} mice, vigorously expanding TCR-tg T cells do not eliminate LCMV from the BM but cause AA very rapidly after infection. This accelerated development of AA illustrates the causal role of the major LCMV-GP-specific effector T cell population in H-2^b mice. Consistent with the general observation that CD4⁺ T cells are not necessary for the induction of antiviral CD8⁺ T effector cells against LCMV (41), CD8⁺ T cell-depleted P^{0/0} mice do not develop AA after LCMV infection. A “compensatory” immunopathologic role for CD4⁺ T cells in mice lacking CD8⁺ CTLs, as has been suggested in meningitis provoked by intracerebral infection of β 2-microglobulin-deficient mice with LCMV (25), is not observed in AA of LCMV-infected P^{0/0} mice.

Cognate Interaction between TCR and Stem Cells versus By-stander Effect. There is no evidence that a precise cell-cell contact between virus-specific CD8⁺ T cells and hematopoietic progenitors presenting a viral epitope on H-2^b is essential for development of AA in LCMV-infected P^{0/0} mice. LCMV persists in high amounts in the BM and colocalizes with stromal and CD11c-positive APCs in BM smears, but virus is not detected in the morphologically defined hematopoietic cells of aplastic P^{0/0} mice. This observation is similar to a previous report, demonstrating LCMV replication in splenic dendritic cells after infection of mice with LCMV clone 13, subsequently leading to generalized immune suppression through elimination of these APCs by virus-specific CTLs (42). Because P^{0/0} mice lack cytotoxic effector functions and therefore cannot kill mesenchymal cells, LCMV-infected APCs in the BM of P^{0/0} mice are not destroyed but support continuous expansion of virus-specific CD8⁺ T cells by serving as an Ag reservoir. Damage by virus-specific T cells and a subsequent early dropout of LCMV-infected stem cells is unlikely to be involved in the pathogenesis of LCMV-induced AA in P^{0/0} mice because lineage-committed progenitors, cultured in vitro at different time points after infection, are free of virus. Loss of tolerance and autoimmunity to progenitors in the BM may be an important mechanism of virus-associated AA in humans (14) and T cell clones, showing autoreactivity to autologous blood cell precursors expressing MHC-DP determinants, have been established (43). As demonstrated in the adoptive transfer experiments, AA in LCMV-infected P^{0/0} mice is not caused by autoimmunity to hematopoietic stem cells in the BM. Taken together, these results implicate that a cognate cell to cell interaction between the TCR of virus-specific CD8⁺ T cells and hematopoietic stem cells either

expressing a LCMV-derived epitope or a cross-reactive self-Ag presented on MHC I, leading to contact-dependent destruction of stem cells, is not involved in AA of LCMV-infected P^{0/0} mice.

Role of TNF/LT- α and IFN- γ . Generation of P^{0/0} mice devoid of the 55-kD TNFR1 gene (P^{0/0}/TNFR1^{0/0} mice) has contributed substantially to the understanding of the mechanism of induction and recovery of AA. In the adult mouse, lack of TNFR1 is not important for clonal deletion of T cells reactive to endogenous viral superantigens and thus, selection of the TCR repertoire is not altered (44). P^{0/0}/TNFR1^{0/0} mice exhibit normal organ sizes of lymphatic tissues, and lymphocyte populations in the thymus and spleen of naive mice are comparable to parental P^{0/0} and TNFR1^{0/0} mice. This suggests normal positive/negative selection of T cells in the absence of both perforin and TNF/LT- α . More important, LCMV titers, expansion of CD8⁺ T cells, Ag specificity, and effector functions via the Fas (CD95)/Fas ligand pathway of virus-specific CD8⁺ T cells are identical in P^{0/0} and P^{0/0}/TNFR1^{0/0} mice. Yet LCMV-infected P^{0/0} mice die of irreversible AA, whereas P^{0/0}/TNFR1^{0/0} mice survive and become virus carriers. They still exhibit BM suppression, although it is quantitatively less severe and reversible after day 14 of LCMV infection. There are two alternative possibilities explaining why TNF/LT- α in LCMV-associated AA is a key molecule deciding on irreversibility of BM failure. (a) TNFR1 is the biologically relevant TNF receptor binding both soluble ligands, TNF and LT- α , by signaling cytotoxicity/apoptosis to many cells, including hematopoietic precursors (28, 45). Injection of TNF into rodents may produce a stimulatory effect on hematopoiesis by induction of colony-stimulating activities in the endothelium (46). In contrast, inhibitory effects of TNF/LT- α on hematopoietic colony formation is well documented in vitro (36). The results in LCMV-infected P^{0/0}/TNFR1^{0/0} mice rather support the interpretation that the ultimate effect of TNF/LT- α activity in virus-associated AA in vivo is suppressive via induction of apoptosis of BM progenitors and is not stimulatory. (b) Alternatively, TNF/LT- α may enhance lymphocyte traffic into the BM by increasing local MHC expression in LCMV-infected dendritic and stromal BM cells. Such a pathway of enhanced CTL-mediated immunopathology has been described in double-tg mice expressing LCMV-GP and TNF in the pancreatic islets (47). The sum of our data supports the first scenario because CD4⁺/CD8⁺ T cell compartments after LCMV infection in the spleen (which is a blood cell-forming tissue in mice) are not altered in the absence of TNFR1. Moreover, the primary foot pad swelling reaction after local infection with LCMV in TNFR1^{0/0} mice is normal, indicating a normal recruitment of virus-specific CTLs into infected tissue (28). We have not assessed the cellular source of the increased TNF/LT- α concentration in the serum of LCMV-infected P^{0/0} mice. However, we have not found TNF/LT- α secretion by LCMV-GP-specific CD8⁺ T cells in vitro. It is conceivable that TNF/LT- α is produced by the monocyte/macrophage system

also in LCMV-infected P^{0/0} mice, as has been found for hepatic macrophages in LCMV-infected hepatitis B virus-transgenic mice (48), or it may be secreted by the stromal matrix of the BM (49).

Depletion experiments with antibodies demonstrate the critical role for IFN- γ -secreting LCMV-GP-specific CD8⁺ T cells, causing AA in LCMV-infected P^{0/0} mice. The following points need to be considered for correct interpretation. (a) IFN- γ exerts a potent inhibitory effect on hematopoietic colony formation in semisolid culture assays in vitro (39, 50) and in long-term cultures, killing via apoptosis and inhibition of cell cycling of stem cells has been found (51). In LCMV-infected P^{0/0} mice, stromal cells in the BM express high amounts of LCMV Ag. However, in contrast to LCMV-infected normal C57BL/6 mice (42), these cells are not eliminated and, therefore, feeder functions of BM stroma are unlikely to be altered, as demonstrated by the virtually normal hematopoiesis in infected P^{0/0} mice lacking both IFN- γ and TNF/LT- α signaling. Furthermore, constitutive expression of IFN- γ in the stromal microenvironment of marrow cultures suppresses progenitor growth in vitro, but seems not to interfere with the expression of hematopoietic growth factor genes such as G-CSF and GM-CSF (51). These observations argue against a stromal defect as cause of AA in LCMV-infected P^{0/0} mice and favor a direct toxic effect of the cytokines for progenitors leading to AA. (b) The results obtained from IFN- γ -depleted P^{0/0} and P^{0/0}/TNFR1^{0/0} mice demonstrate that IFN- γ is more potent in suppressing hematopoiesis than TNF/LT- α . This may be in contrast to the synergistic inhibitory effect of IFN- γ and TNF/LT- α that has been documented on colony formation in vitro (36). The dissimilarity to these in vitro findings is best explained by the sustained expansion of IFN- γ -secreting CD8⁺ T cells in the presence of persisting LCMV in aplastic P^{0/0} mice and rather reflects the kinetics of the immune response than the toxic potential of TNF/LT- α versus that of IFN- γ . It will be interesting to study whether TNF/LT- α production in macrophages is diminished in the absence of IFN- γ in LCMV-infected P^{0/0} mice, because IFN- γ is known to induce expression of TNF/LT- α in these cells (52). (c) IFN- γ exerts important effects on MHC I/II expression and thereby influences Ag presentation (53). Recent data has shown that IFN- γ knockout mice generate LCMV-specific primary CTLs with equivalent activities and terminate acute LCMV infection as efficiently as normal control mice (16, 54). This finding and the typical inversion of CD4⁺/CD8⁺ T cells in spleens of IFN- γ -depleted, LCMV-infected P^{0/0} mice, excludes an insufficient induction of virus-specific CD8⁺ T cells being involved in improvement of hematopoietic function in the absence of IFN- γ . (d) In LCMV-infected P^{0/0}/TNFR1^{0/0} mice, residual BM suppression is reversible and BM function is rescued after IFN- γ -secreting CD8⁺ T cells have disappeared. Because CD8⁺ T cells of P^{0/0}/TNFR1^{0/0} mice lack functional TNF/LT- α signaling, this finding argues against a distinct role for TNF/LT- α in tolerance induction by functional exhaustion of LCMV-spe-

cific CTLs leading to viral persistence. This is in contrast to a recent report, demonstrating a delayed deletion of LCMV-specific TCR-tg CTLs in an adoptive transfer system (55). In the latter study, an LCMV-GP-derived peptide was administered and, therefore, the critical threshold of Ag concentration and distribution, as well as sustained presentation of the Ag on MHC I, required for exhaustive activation of virus-specific CTLs, has probably not been achieved. Thus, the close correlation of kinetics between BM recovery and functional exhaustion of LCMV-specific CD8⁺ T cells emphasizes the causal role of CD8⁺ T cell-dependent IFN- γ in LCMV-induced AA. (e) Even overwhelming IFN- γ secretion is not sufficient to reduce viral titers in the BM of LCMV-infected P^{0/0} mice. This is in contrast to HBV-specific CTLs, which have been shown to abolish HBV replication in the liver of tg mice via secretion of TNF/LT- α and IFN- γ . Damage of the hepatocyte did not follow Ag recognition and CTL-dependent cytokine secretion (56). This apparent discrepancy to LCMV-associated AA may reflect the difference of the cell cycling conditions in hematopoietic tissue, i.e., regularly dividing pluripotent and committed stem cells are likely to be more susceptible to locally secreted cytokines than hepatocytes.

Relevance to Virus-associated Aplastic Anemia in Humans

Virus-associated AA in humans and in LCMV-infected P^{0/0} mice differ in several details that need to be explained. Clinically, pancytopenia in human AA presents gradually, usually 1–7 wk after an episode of acute hepatitis (8). In contrast, LCMV-infected P^{0/0} mice exhibit very rapid kinetics of blood cell depression and BM failure. The influence of a relatively high LCMV dose applied intravenously to inbred mice fostered in an SPF environment may partially account for the aggressive disease development. More important, P^{0/0} mice are an exceptional example of a virus host relationship because P^{0/0} mice cannot control LCMV replication, and therefore high viral titers are reached very early after infection. Additionally, the rapid progression to lethal AA may be due to an intrinsic difference in the kinetics and turnover of hematopoietic cells in mice versus humans (e.g., a higher proportion of mouse stem cells are in the cell cycle). Particularly, the low granulocyte count in mice of the C57BL/6 background and the shorter life span of erythrocytes and platelets may contribute to the rapid time course of the disease. It is noteworthy, that assessment of CFU-S on day 12 does not reflect the frequency of the repopulating cell in mice, i.e., the pluripotent stem cell. However, depletion of these most primitive stem cells in aplastic P^{0/0} mice may be inferred from the results obtained from the CBCs, the culture data, and the content of CFU-S in the BM. Furthermore, loss of CFU-S in LCMV-infected P^{0/0} mice appears to sufficiently reflect the human phenotype because the point of injury in virus-associated AA in humans is probably distal to the most primitive stem cell, suggested by the normal number and maintenance of other stem cell-derived compartments such as lymphocytes and osteoclasts in these patients (2).

Systemic Activation of Virus-specific CTLs. Lacking the most important CTL effector function for LCMV elimination, $P^{0/0}$ mice are, in a certain way, immunodeficient animals. In $P^{0/0}$ mice, LCMV replicates in many mesenchymal and epithelial cells, leading to systemic expansion of $CD8^+$ T cells not only in the BM, but also in other organs (liver, brain, etc.). Due to lack of contact-dependent cytotoxicity of virus-specific $CD8^+$ T cells, necrosis of tissue and solid organ disease is absent (27). Virus-associated human AA is dissimilar in that respect because hepatitis is usually prevalent in individuals with a normal immune status and it is thought that damaging CTLs localize more specifically to the BM in the course of the disease (8). However, observations in wt C57BL/6 mice limit the interpretation of AA in $P^{0/0}$ mice only with respect to disease intensity and kinetics for the following reasons. Similar to $P^{0/0}$ mice, suppression of BM function is also seen in wt C57BL/6 mice with a latency of ~ 1 wk (days 16–22) after LCMV-induced hepatitis when the correct viral inoculation dose and LCMV strain is chosen (LCMV-Docile, 10^4 PFU). Although $\sim 10\%$ of infected mice die, LCMV infection does not cause AA consistently in C57BL/6 mice and most animals show only a mild decrease of the CBCs that is transient and reversible after LCMV has been cleared.

Cytokine Profile of CTLs. A remarkable discordance is observed in the profile of secreted cytokines by $CD8^+$ T cells; in contrast to T cells of patients with AA, overproduction of TNF/LT- α by LCMV-specific CTLs is not detected, although TNF/LT- α concentrations in serum of LCMV-infected $P^{0/0}$ and $P^{0/0}/TNFR1^{0/0}$ mice are increased. Because the viral Ags are not known, human T cell clones obtained by stimulation of BM cells with lectins usually exhibit strong NK activity in vitro (40). Thus, TNF/LT- α release in these experiments may not directly reflect a product of MHC-restricted T cells, but could be due to an enhanced release from secondary cells, such as NK cells, induced via IFN- γ from virus-specific CTLs (52). In contrast, cytokine secretion in LCMV-infected $P^{0/0}$ mice is highly Ag specific and MHC restricted because only $CD8^+$ T cells recognizing the immunodominant epitope derived from LCMV-GP presented on H-2^b secrete IFN- γ .

Other Models of AA. Currently, there is no murine model describing an irreversible BM aplasia caused by virus-specific $CD8^+$ T cells that exhibits disease characteristics comparable to human virus-associated AA. Immunologically mediated AA can be induced experimentally in irradiated recipient mice by infusion of lymph node cells from H-2-syngeneic but Mls-mismatched donors (57). In another system, small doses of purified unprimed $CD4^+$ cells are transferred into lightly irradiated recipients expressing

MHC class II (I-A) differences. The donor $CD4^+$ cells cause destruction of the BM and it has been concluded that $CD4^+$ T cells induce AA via I-A-restricted CTL activity through recognition of I-A expression on stem cells (58). Both disease models, however, correspond best to BM aplasia as a consequence of a chronic graft versus host disease and therefore, the mechanism of development of disease may be dissimilar from virus-associated AA in humans.

Implications for Human AA. LCMV-infected $P^{0/0}$ mice seem a valid system to explore the pathogenesis of virus-associated AA, the natural course of the disease, and the conditions allowing its spontaneous recovery. Because the disease incidence is 100% with a highly predictable time course not only in tg, but also in non-tg animals, the contribution of distinct subpopulations of virus-specific lymphocytes to disease can clearly be dissected. In addition, mice are the natural host and reservoir of LCMV (29, 59). Therefore, the mechanism of disease described here may offer explanations for hematopoietic disease also in other arenavirus infections such as Junin and Tamiami viruses, in which destruction and widespread loss of hematopoietic tissue is observed (60). The network of growth factors and inhibitors that governs proliferation and maturation of hematopoietic cells is very complex due to synergistic, overlapping and counterregulatory bioactivities of cytokines. Additional inhibitory factors produced by BM stroma (e.g., macrophage inflammatory protein [MIP]-1 α [61] or TGF- β [62]) may be involved in AA of LCMV-infected $P^{0/0}$ mice and have not been studied here. Our experiments suggest that progressive BM failure and functional exhaustion of virus-specific $CD8^+$ T cells are ruled by distinct pathogenetic mechanisms during persistent virus infections. Consequently, in virus-induced AA, the final outcome of a life-long virus carrier state or mortality of the host may be the result of a mutual competition between loss of the hematopoietic stem cells versus loss of damaging virus-specific T cells. Absence of one toxic $CD8^+$ T cell-dependent cytokine, such as TNF/LT- α or IFN- γ , shifts this lethal balance and rescues BM function. This mechanism of peripheral tolerance induction may explain why rare patients survive AA and remission to normal blood cell values can “naturally” occur (2). Persistent expression of viral Ag in stromal and dendritic cells in the spatially limited microenvironment of the BM efficiently sustains local infiltration with $CD8^+$ T cells and causes AA via bystander destruction of blood cell precursors by T cell-secreted cytokines. These concepts of nonbalanced antiviral immunity causing hematopoietic disease may possibly be generalized to other viruses that are noncytopathic for blood cell progenitors and predominantly infect the stroma (5, 6) or other, not yet defined cellular targets in the BM (8, 9).

We are grateful to A. Althage, E. Horvath, and R. Rüegg for excellent technical assistance, and to N. Wey for processing the photographs. We thank P. Aichele, P. Klenerman, and H. Pircher for helpful discussions. Recombinant mTPO was kindly provided as a gift by Genentech, Inc. (South San Francisco, CA).

This work was supported by the Union Bank of Switzerland, the Swiss National Science Foundation, the Kanton of Zürich, and the ETH Zürich.

Received for publication 6 March 1998.

References

1. Kagan, W.A., J.A. Ascensao, R.N. Pahwa, J.A. Hansen, G. Goldstein, E.B. Valera, G.S. Incefy, M.A. Moore, and R.A. Good. 1976. Aplastic anemia: presence in human bone marrow of cells that suppress myelopoiesis. *Proc. Natl. Acad. Sci. U.S.A.* 73:2890-2894.
2. Young, N.S., and B.P. Alter. 1994. Aplastic anemia: acquired and inherited. W.B. Saunders, Philadelphia. 1-267.
3. Iishi, Y., M. Kosaka, T. Mizuguchi, K. Toyota, Y. Takaue, Y. Kawano, and S. Saito. 1991. Suppression of hematopoiesis by activated T-cells in infectious mononucleosis associated with pancytopenia. *Int. J. Hematol.* 54:65-73.
4. Shadduck, R.K., A. Winkelstein, Z. Zeigler, J. Lichter, M. Goldstein, M. Michaels, and B. Rabin. 1979. Aplastic anemia following infectious mononucleosis: possible immune etiology. *Exp. Hematol. (NY)*. 7:264-271.
5. Apperley, J.F., C. Dowding, J. Hibbin, J. Buiter, E. Matutes, P.J. Sissons, M. Gordon, and J.M. Goldman. 1989. The effect of cytomegalovirus on hemopoiesis: in vitro evidence for selective infection of marrow stromal cells. *Exp. Hematol. (NY)*. 17:38-45.
6. Reddehase, M.J., L. Dreher-Stumpp, P. Angele, M. Baltheisen, and M. Susa. 1992. Hematopoietic stem cell deficiency resulting from cytomegalovirus infection of bone marrow stroma. *Ann. Hematol.* 64:A125-A127.
7. Molina, J.-M., D.T. Scadden, M. Sakaguchi, B. Fuller, A. Woon, and J.E. Grooman. 1990. Lack of evidence for infection of or effect on growth of hematopoietic progenitor cells after in vivo or in vitro exposure to human immunodeficiency virus. *Blood*. 76:2476-2482.
8. Brown, K.E., J. Tisdale, A.J. Barrett, C.E. Dunbar, and N.S. Young. 1997. Hepatitis-associated aplastic anemia. *N. Engl. J. Med.* 336:1059-1064.
9. Tzakis, A.G., M. Ardit, P.F. Whittington, K. Yanaga, C. Esquivel, W.A. Andrews, L. Makowka, J. Malatak, D.K. Freese, and P.G. Stock. 1988. Aplastic anemia complicating orthotopic liver transplantation for non-A, non-B hepatitis. *N. Engl. J. Med.* 319:393-396.
10. Albert, E., E.D. Thomas, B. Nispersos, and R. Storb. 1976. HLA antigens and haplotypes in 200 patients with aplastic anemia. *Transplantation*. 22:528-531.
11. Chapuis, B., V.E. Von Flidner, M. Jeannet, H. Merica, P. Vuagnat, A. Gratwohl, C. Nissen, and B. Speck. 1986. Increased frequency of DR2 in patients with aplastic anaemia and increased DR sharing in their parents. *Br. J. Haematol.* 63:51-57.
12. Speck, B., A. Gratwohl, C. Nissen, U. Leibundgut, D. Ruggero, B. Osterwalder, H.P. Burri, P. Cornu, and M. Jeannet. 1981. Treatment of severe aplastic anaemia with antilymphocyte globulin or bone-marrow transplantation. *Br. Med. J.* 282:860-863.
13. Thomas, E.D., R. Storb, A. Fefer, S.J. Slichter, J.I. Bryant, C.D. Buckner, P.E. Neiman, R.A. Clift, D.D. Funk, and K.E. Lerner. 1972. Aplastic anaemia treated by marrow transplantation. *Lancet*. 1:284-289.
14. Young, N.S., and J. Maciejewski. 1997. The pathophysiology of acquired aplastic anemia. *New. Engl. J. Med.* 336:1365-1372.
15. Binder, D., J. Fehr, H. Hengartner, and R.M. Zinkernagel. 1997. Virus-induced transient bone marrow aplasia: major role of interferon-alpha/beta during acute infection with the noncytotoxic lymphocytic choriomeningitis virus. *J. Exp. Med.* 185:517-530.
16. Müller, U., U. Steinhoff, L.F.L. Reis, S. Hemmi, J. Pavlovic, R.M. Zinkernagel, and M. Aguet. 1994. Functional role of type I and type II interferons in antiviral defense. *Science*. 264:1918-1921.
17. Aichele, P., M.F. Bachmann, H. Hengartner, and R.M. Zinkernagel. 1996. Immunopathology or organ-specific autoimmunity as a consequence of virus infection. *Immunol. Rev.* 152:21-45.
18. Cole, G.A., N. Nathanson, and R.A. Prendergast. 1972. Requirement for theta-bearing cells in lymphocytic choriomeningitis virus-induced central nervous system disease. *Nature*. 238:335-337.
19. Zinkernagel, R.M., E. Haenseler, T. Leist, A. Cerny, H. Hengartner, and A. Althage. 1986. T cell-mediated hepatitis in mice infected with lymphocytic choriomeningitis virus. *J. Exp. Med.* 164:1075-1092.
20. Leist, T.P., E. Rüedi, and R.M. Zinkernagel. 1988. Virus-triggered immune suppression in mice caused by virus-specific cytotoxic T cells. *J. Exp. Med.* 167:1749-1754.
21. Kägi, D., B. Odermatt, P.S. Ohashi, R.M. Zinkernagel, and H. Hengartner. 1996. Development of insulinitis without diabetes in transgenic mice lacking perforin-dependent cytotoxicity. *J. Exp. Med.* 183:2143-2152.
22. Evans, C.F., M.S. Horwitz, M.V. Hobbs, and M.B. Oldstone. 1996. Viral infection of transgenic mice expressing a viral protein in oligodendrocytes leads to chronic central nervous system autoimmune disease. *J. Exp. Med.* 184:2371-2384.
23. Hotchin, J. 1962. The biology of lymphocytic choriomeningitis infection: virus induced immune disease. *Cold Spring Harbor Symp. Quant. Biol.* 27:479-499.
24. Pfau, C.J., J.K. Valenti, D.C. Pevear, and K.D. Hunt. 1982. Lymphocytic choriomeningitis virus killer T cells are lethal only in weakly disseminated murine infections. *J. Exp. Med.* 156:79-89.
25. Muller, D., B.H. Koller, J.L. Whitton, K.E. LaPan, K.K. Brigman, and J.A. Frelinger. 1992. LCMV-specific, class II-restricted cytotoxic T cells in beta 2-microglobulin-deficient mice. *Science*. 255:1576-1578.
26. Harrison, D.E., C.M. Astle, and C. Lerner. 1988. Number and continuous proliferative pattern of transplanted primitive immunohematopoietic stem cells. *Proc. Natl. Acad. Sci. U.S.A.* 85:822-826.
27. Kägi, D., B. Ledermann, K. Bürki, P. Seiler, B. Odermatt, K.J. Olsen, E.R. Podack, R.M. Zinkernagel, and H. Hengartner. 1994. Cytotoxicity mediated by T cells and natural

- killer cells is greatly impaired in perforin-deficient mice. *Nature*. 369:31–37.
28. Rothe, J., W. Lesslauer, H. Lotscher, Y. Lang, P. Koebel, F. Kontgen, A. Althage, R. Zinkernagel, M. Steinmetz, and H. Bluethmann. 1993. Mice lacking the tumour necrosis factor receptor 1 are resistant to TNF-mediated toxicity but highly susceptible to infection by *Listeria monocytogenes*. *Nature*. 364: 798–802.
 29. Lehmann-Grube, F. 1971. Lymphocytic choriomeningitis virus. *Monogr. Virol.* 10:1–173.
 30. Battegay, M., S. Cooper, A. Althage, J. Baenziger, H. Hengartner, and R.M. Zinkernagel. 1991. Quantification of lymphocytic choriomeningitis virus with an immunological focus assay in 24 or 96 well plates. *J. Virol. Methods*. 33:191–198.
 31. Cobbold, S.P., A. Jayasuriya, A. Nash, T.D. Prospero, and H. Waldmann. 1984. Therapy with monoclonal antibodies by elimination of T-cell subsets in vivo. *Nature*. 312:548–551.
 32. Leist, T.P., M. Eppler, and R.M. Zinkernagel. 1989. Enhanced virus replication and inhibition of lymphocytic choriomeningitis disease in anti-gamma interferon-treated mice. *J. Virol.* 63:2813–2819.
 33. Zinkernagel, R.M., T.P. Leist, H. Hengartner, and A. Althage. 1985. Susceptibility to lymphocytic choriomeningitis virus isolates correlates directly with early and cytotoxic T cell activity, as well as with footpad swelling reaction, and all three are regulated by H-2D. *J. Exp. Med.* 162:2125–2141.
 34. Pruslin, F.H. 1991. Caveats and suggestions for the ELISA. *J. Immunol. Methods*. 137:27–35.
 35. Kägi, D., B. Ledermann, K. Bürki, R.M. Zinkernagel, and H. Hengartner. 1995. Lymphocyte-mediated cytotoxicity in vitro and in vivo: mechanisms and significance. *Immunol. Rev.* 146:95–115.
 36. Murphy, M., R. Loudon, M. Kobayashi, and G. Trinchieri. 1986. Gamma-interferon and lymphotoxin released by activated T cells synergize to inhibit granulocyte/monocyte colony formation. *J. Exp. Med.* 164:263–279.
 37. Zoumbos, N.C., W.O. Ferris, S.M. Hsu, S. Goodman, P. Griffith, S.O. Sharrow, R.K. Humphries, A.W. Nienhuis, and N. Young. 1984. Analysis of lymphocyte subsets in patients with aplastic anaemia. *Br. J. Haematol.* 58:95–105.
 38. Nakao, S., M. Yamaguchi, S. Shiobara, T. Yokoi, T. Miyawaki, T. Taniguchi, and T. Matsuda. 1992. Interferon-gamma gene expression in unstimulated bone marrow mononuclear cells predicts a good response to cyclosporine therapy in aplastic anemia. *Blood*. 79:2532–2535.
 39. Zoumbos, N.C., P. Gascon, J.Y. Djeu, and N.S. Young. 1985. Interferon is a mediator of hematopoietic suppression in aplastic anemia in vitro and possibly in vivo. *Proc. Natl. Acad. Sci. U.S.A.* 82:188–192.
 40. Viale, M., A. Merli, and A. Bacigalupo. 1991. Analysis at the clonal level of T-cell phenotype and functions in severe aplastic anemia patients. *Blood*. 78:1268–1274.
 41. Ahmed, R., A. Salmi, L.D. Butler, J.M. Chiller, and M.B. Oldstone. 1984. Selection of genetic variants of lymphocytic choriomeningitis virus in spleens of persistently infected mice. Role in suppression of cytotoxic T lymphocyte response and viral persistence. *J. Exp. Med.* 160:521–540.
 42. Borrow, P., C.F. Evans, and M.B. Oldstone. 1995. Virus-induced immunosuppression: immune system-mediated destruction of virus-infected dendritic cells results in generalized immune suppression. *J. Virol.* 69:1059–1070.
 43. Moebius, U., F. Herrmann, T. Hercend, and S.C. Meuer. 1991. Clonal analysis of CD4+/CD8+ T cells in a patient with aplastic anemia. *J. Clin. Invest.* 87:1567–1574.
 44. Pfeffer, K., T. Matsuyama, T.M. Kundig, A. Wakeham, K. Kishihara, A. Shahinian, K. Wiegmann, P.S. Ohashi, M. Kronke, and T.W. Mak. 1993. Mice deficient for the 55 kd tumor necrosis factor receptor are resistant to endotoxic shock, yet succumb to *L. monocytogenes* infection. *Cell*. 73: 457–467.
 45. Tartaglia, L.A., and D.V. Goeddel. 1992. Two TNF receptors. *Immunol. Today*. 13:151–153.
 46. Johnson, C.S., M.J. Chang, and P. Furmanski. 1988. In vivo hematopoietic effects of tumor necrosis factor- α in normal and erythroleukemic mice: characterization and therapeutic applications. *Blood*. 72:1875–1883.
 47. Ohashi, P.S., S. Oehen, P. Aichele, H. Pircher, B. Odermatt, P. Herrera, Y. Higuchi, K. Buerki, H. Hengartner, and R.M. Zinkernagel. 1993. Induction of diabetes is influenced by the infectious virus and local expression of MHC class I and tumor necrosis factor- α . *J. Immunol.* 150:5185–5194.
 48. Guidotti, L.G., P. Borrow, M.V. Hobbs, B. Matzke, I. Gresser, M.B. Oldstone, and F.V. Chisari. 1996. Viral cross talk: intracellular inactivation of the hepatitis B virus during an unrelated viral infection of the liver. *Proc. Natl. Acad. Sci. U.S.A.* 93:4589–4594.
 49. Sieff, C.A., C.M. Niemeyer, S.J. Mentzer, and D.V. Faller. 1988. Interleukin-1, tumor necrosis factor, and the production of colony-stimulating factors by cultured mesenchymal cells. *Blood*. 72:1316–1323.
 50. Broxmeyer, H.E., L. Lu, E. Platzer, C. Feit, L. Juliano, and B.Y. Rubin. 1983. Comparative analysis of the influences of human gamma, alpha and beta interferons on human multipotential (CFU-GEMM), erythroid (BFU-E) and granulocyte-macrophage (CFU-GM) progenitor cells. *J. Immunol.* 131:1300–1305.
 51. Selleri, C., J.P. Maciejewski, T. Sato, and N.S. Young. 1996. Interferon-gamma constitutively expressed in the stromal microenvironment of human marrow cultures mediates potent hematopoietic inhibition. *Blood*. 87:4149–4157.
 52. Collart, M.A., D. Belin, J.D. Vassalli, S. de Kossodo, and P. Vassalli. 1986. Gamma interferon enhances macrophage transcription of the tumor necrosis factor/cachectin, interleukin 1, and urokinase genes, which are controlled by short-lived repressors. *J. Exp. Med.* 164:2113–2118.
 53. Collins, T., A.J. Korman, C.T. Wake, J.M. Boss, D.J. Kappes, W. Fiers, K.A. Ault, M.A. Gimbrone, Jr., J.L. Strominger, and J.S. Pober. 1984. Immune interferon activates multiple class II major histocompatibility complex genes and the associated invariant chain gene in human endothelial cells and dermal fibroblasts. *Proc. Natl. Acad. Sci. U.S.A.* 81: 4917–4921.
 54. Huang, S., W. Hendriks, A. Althage, S. Hemmi, H. Bluethmann, R. Kamijo, J. Vilcek, R.M. Zinkernagel, and M. Aguet. 1993. Immune response in mice that lack the interferon-gamma receptor. *Science*. 259:1742–1745.
 55. Speiser, D.E., E. Sebza, T. Ohteki, M.F. Bachmann, K. Pfeffer, T.W. Mak, and P.S. Ohashi. 1996. Tumor necrosis factor receptor p55 mediates deletion of peripheral cytotoxic T lymphocytes in vivo. *Eur. J. Immunol.* 26:3055–3060.
 56. Guidotti, L.G., T. Ishikawa, M.V. Hobbs, B. Matzke, R. Schreiber, and F.V. Chisari. 1996. Intracellular inactivation of the hepatitis B virus by cytotoxic T lymphocytes. *Immunity*. 4:25–36.

57. Knospe, W.H., D. Steinberg, and B. Speck. 1983. Experimental immunologically mediated aplastic anemia (AA) in H-2k identical, Mls (M) locus different mice. *Exp. Hematol. (NY)*. 11:542-552.
58. Sprent, J., C.D. Surh, D. Agus, M. Hurd, S. Sutton, and W.R. Heath. 1994. Profound atrophy of the bone marrow reflecting major histocompatibility complex class II-restricted destruction of stem cells by CD4+ cells. *J. Exp. Med.* 180:307-317.
59. Hotchin, J.E. 1971. Persistent and slow virus infections. *Monogr. Virol.* 3:1-211.
60. Peralta, L.A.M., C.E. Coto, and M.C. Weissenbacher. 1993. The Tacaribe complex: the close relationship between a pathogenic (junin) and a nonpathogenic (tacaribe) arenavirus. *In The Arenaviridae*. M.S. Salvato, editor. Plenum Press, New York. 281-298.
61. Holmberg, L.A., K. Seidel, W. Leisenring, and B. Torok-Storb. 1994. Aplastic anemia: analysis of stromal cell function in long-term marrow cultures. *Blood.* 84:3685-3690.
62. Cashman, J.D., A.C. Eaves, E.W. Raines, R. Ross, and C.J. Eaves. 1990. Mechanisms that regulate the cell cycle status of very primitive hematopoietic cells in long-term human marrow cultures. I. Stimulatory role of a variety of mesenchymal cell activators and inhibitory role of TGF-beta. *Blood.* 75: 96-101.